^{40}Ar/^{39}Ar and field studies of Quaternary basalts in Grand Canyon and model for carving Grand Canyon: Quantifying the interaction of river incision and normal faulting across the western edge of the Colorado Plateau

Karl E. Karlstrom*
Ryan S. Crow
Department of Earth and Planetary Sciences, University of New Mexico, Albuquerque, New Mexico 87131, USA

Lisa Peters
William McIntosh
New Mexico Bureau of Geology and Mineral Technology, Geochronology Lab, 801 Leroy Place, New Mexico Institute of Technology, Socorro, New Mexico 87801, USA

Jason Raucci
Department of Geology, 4099, Northern Arizona University, Flagstaff, Arizona 86011, USA

Laura J. Crossey
Department of Earth and Planetary Sciences, University of New Mexico, Albuquerque, New Mexico 87131, USA

Paul Umhoefer
Department of Geology, 4099, Northern Arizona University, Flagstaff, Arizona 86011, USA

Nelia Dunbar
New Mexico Bureau of Geology and Mineral Technology, Geochronology Lab, 801 Leroy Place, New Mexico Institute of Technology, Socorro, New Mexico 87801, USA

ABSTRACT

^{40}Ar/^{39}Ar dates on basalts of Grand Canyon provide one of the best records in the world of the interplay among volcanism, differential canyon incision, and neotectonic faulting. Earlier ^{40}K/^{40}Ar dates indicated that Grand Canyon had been carved to essentially its present depth before 1.2 Ma. But new ^{40}Ar/^{39}Ar data cut this time frame approximately in half; new ages are all <723 ka, with age probability peaks at 606, 534, 348, 192, and 102 ka. Strategic sampling of basalts provides a semicontinuous record for deciphering late Quaternary incision and fault-slip rates and indicates that basalts flowed into and preserved a record of a progressively deepening bedrock canyon.

The Eastern Grand Canyon block (east of Toroweap fault) has bedrock incision rates of 150–175 m/Ma over approximately the last 500 ka; western Grand Canyon block (west of Hurricane fault) has bedrock incision rates of 50–75 m/Ma over approximately the last 720 ka. Fault displacement rates are 97–106 m/Ma on the Toroweap fault (last 500–600 ka) and 70–100 m/Ma on the Hurricane fault (last 200–300 ka). As the river crosses each fault, the apparent incision rate is lowest in the immediate hanging wall, and this rate, plus the displacement rate, is subequal to the incision rate in the footwall. At the reach scale, variation in apparent incision rates delineates ~100 m/Ma of cumulative relative vertical lowering of the western Grand Canyon block relative to the eastern block and 70–100 m of slip accommodated by formation of a hanging-wall anticline.

Data from the Lake Mead region indicate that our refined fault-dampened incision model has operated over the last 6 Ma. Bedrock incision rate has been 20–30 m/Ma in the lower Colorado River block in the last 5.5 Ma, and displacement on the Wheeler fault has resulted in both lowering of the Lower Colorado River block and formation of a hanging-wall anticline of the 6-Ma Hualapai Limestone. In modeling long-term incision history, extrapolation of Quaternary fault displacement and incision rates linearly back 6 Ma only accounts for approximately two-thirds of eastern and approximately one-third of western Grand Canyon incision. This "incision discrepancy" for carving Grand Canyon is best explained by higher rates during early (5- to 6-Ma) incision in eastern Grand Canyon and the existence of Miocene paleocanyons in western Grand Canyon.

Differential incision data provide evidence for relative vertical displacement across Neogene faults of the Colorado Plateau-Basin and Range transition, a key data set for evaluating uplift and incision models. Our data indicate that the Lower Colorado River block has lowered 25–50 m/Ma (150–300 m) relative to the western Grand Canyon block and 125–150 m/Ma (750–900 m) relative to the eastern Grand Canyon block in 6 Ma. The best model explaining the constrained reconstruction of the 5- to 6-Ma Colorado River paleoprofile, and other geologic data, is that most of the 750–900 m of relative vertical block motion that accompanied canyon

*kek1@unm.edu

incision was due to Neogene surface uplift of the Colorado Plateau.

Keywords: Grand Canyon, river incision, Ar-Ar dating, Quaternary basalts, tectonic geomorphology.

INTRODUCTION: BACKGROUND AND GOALS

In spite of over a century of work on the Grand Canyon, there are still fundamental questions about the age of the canyon and the processes that have formed it. There is consensus (e.g., Young and Spamer, 2001) that the present Colorado River system through Grand Canyon took its shape only in the last 6 Ma, ca. 65 Ma after Laramide uplift of the Colorado Plateau and 10–20 Ma after the Sevier/Laramide highlands collapsed to form the Basin and Range province in the Miocene. Miocene topographic inversion left the Colorado Plateau higher, reversed some drainages (Potochnik, 2001), and created significant fault scarps at the western edge of the Colorado Plateau, but the Colorado River did not become integrated across the Kaibab Plateau and through western Grand Canyon until after deposition of the Hualapai Limestone (ending 5.97 ± 0.07 Ma; Spencer et al., 2001). Carving of Grand Canyon began after 6 Ma due to integration of a river system that took drainage from the elevated Colorado Plateau, through basins in the Basin and Range province, to a lowered base level in the Gulf of California that began opening 6.5–6.3 Ma (McDougall et al., 1999; Oskin and Stock, 2003). Sediments from the Colorado Plateau first reached the Gulf of California 5.36 ± 0.06 Ma (Dorsey et al., 2005), marking a Colorado River system that had achieved approximately its present course (Fig. 1). By 4.41 ± 0.03 Ma (Faulds et al., 2001), basalts at Sandy Point on Lake Mead (Fig. 1) were emplaced on top of Colorado River gravels in a paleochannel in about the same place as the modern channel.

For the critical period 5–10 Ma, there are few deposits and no accurate paleoelevation data. For this time period, major uncertainties include: (1) the relative importance of headward erosion from the Gulf to drive incision across the Grand Wash cliffs onto the Colorado Plateau (Lucchitta, 1972, 1979, 1990; Buising, 1990; Lucchitta et al., 2001) versus lake spill over and integration from the plateau downward (Spencer and Patchett, 1997; Faulds et al., 2001; Meek and Douglas, 2001; Spencer and Pearthree, 2001; House et al., 2005); (2) the role of Neogene surface uplift of the Colorado Plateau (Lucchitta et al., 2001; Sahagian et al., 2002), if any (Spencer and Patchett, 1997; Spencer et al., 2001; Patchett and Spencer, 2001; Pederson et al., 2002a);

(3) relative vertical displacement and timing of movements of normal faults near the Colorado Plateau-Basin and Range boundary and their effect on incision processes (Hamblin et al., 1981; Willis and Biek, 2001; Pederson and Karlstrom, 2001); and (4) the depth and shape of pre–6-Ma paleocanyons that may have been reused, linked, and deepened in the process of carving Grand Canyon (Young, 2001, 2007).

Datable basalts of the western Grand Canyon offer the opportunity to better constrain the incision of Grand Canyon and to understand the neotectonic and geomorphic interactions of volcanism, canyon incision, and normal faulting. The Uinkaret volcanic field (Fig. 1; Uinkaret Plateau block of Beus and Morales, 2003) is a north-south–trending field of cinder cones and basalt flows that is situated between the Hurricane and Toroweap faults (Fig. 1). Although some vents existed within Grand Canyon, basalt flowed into Grand Canyon mainly from the north rim, with some flows traveling >120 km down the river corridor (from RM 179–254[1]; Fig. 1). Flows on the Uinkaret Plateau range in age from 3.4 to 3.7 Ma on Mount Trumbull ($^{40}K/^{40}Ar$; Best et al., 1980; Billingsley, 2001) to ca. 1 ka (Fenton et al., 2001). But, as reported here, intracanyon basalt flows range from ca. 700 to ca. 100 ka.

The first goal of this paper is to present new $^{40}Ar/^{39}Ar$ dates on basalts from western Grand Canyon (Fig. 2). The new $^{40}Ar/^{39}Ar$ dates offer a significant advance over both $^{40}K/^{40}Ar$ dates, which tend to be too old because of undetected excess ^{40}Ar, and cosmogenic surface ages, which tend to be too young due to degradation of surfaces. The $^{40}Ar/^{39}Ar$ method, coupled with sample characterization and preparation techniques designed to recognize and remove incorporated clays, allows us to eliminate the elevated ages seen at high-and/or low-temperature steps and arrive at a better estimate of the eruption age (Fig. 3).

The second goal of this paper is to use the new geochronologic data to provide better estimates of Quaternary incision history of Grand Canyon. Earlier workers thought that Grand Canyon had been deepened to essentially its present depth before 1.2 Ma based on $^{40}K/^{40}Ar$ dates (Hamblin, 1970b, 1974, 1994), but new $^{40}Ar/^{39}Ar$ data and incision studies presented here indicate that basalts flowed into and preserved a record of a progressively deepening bedrock canyon. This incision is recorded by basalt remnants in the

river corridor that overlie river gravels, which, in turn, rest on top of elevated bedrock straths. This paper presents new, high-quality, incision-rate points, along with a comprehensive summary of published incision-rate data.

The third goal of this paper is to understand the interaction of canyon incision with active normal faulting and refine the model of fault-dampened incision first presented by Pederson and Karlstrom (2001) and Pederson et al. (2002b). Various workers have noted that canyon incision, basaltic volcanism, and extensional faulting have all interacted (Hamblin et al., 1981; Jackson, 1990; Stenner et al., 1999; Fenton et al., 2001; Pederson et al., 2002b); this paper offers a synthesis of these interacting processes, and their rates, based on new geochronology and field studies. The refined differential incision model presented in this paper quantifies the relative roles of vertical-block motion versus hanging-wall flexure in causing lowered apparent incision rates as the river crosses several west-down Neogene normal faults.

The last part of the paper applies the differential incision data to develop a model for the long-term incision history of Grand Canyon. We combine incision rates, fault displacement rates, slip durations on different faults, and differential-incision patterns to extend the differential incision model back to 6 Ma. Differential incision due to faulting was an important process throughout the Neogene tectonic development of the Colorado Plateau-Basin and Range transition and one that has been left out of most models for carving Grand Canyon.

$^{40}Ar/^{39}Ar$ Results

We performed a total of 63 incremental, step-heating analyses at the New Mexico Tech Geochronology Research Laboratory on 44 Grand Canyon basalt samples collected mainly during 2000 and 2001 (Figs. 2 and 4; Table 1; Table DR1)[2]. Twenty-six samples (based on 44 analyses) yielded reliable new dates (2 sigma error <±150 ka) that we interpret to be accurate eruption ages (Fig. 2; Table 1). The characterization of samples by electron microprobe has been critical for successful dating, both for identifying the most promising samples, and for guiding preparation and treatment of problem samples. Microprobe observations reveal variable amounts of matrix glass, alteration of glass or phenocrysts, and/or abundant clay (Fig. 3), unusual for late Quaternary basaltic lavas in arid

---

[1] For locations throughout this paper, we use conventional nomenclature of river miles (RM) downstream from Lees Ferry, using Stevens's (1983) river miles. The river profiles, showing elevations of the river surface, are from the detailed Birdsey survey (1924), with bathymetry added from sonar studies of Wilson (1986), and a schematic representation of geologic units modified from Moores (in LaRue, 1925).

[2] GSA Data Repository Item 2007263, Table DR1 ($^{40}Ar/^{39}Ar$ analytical data) and Table DR2 (displacements across major faults and of fault-slip rates), is available at www.geosociety.org/pubs/ft2007.htm. Requests may also be sent to editing@geosociety.org.
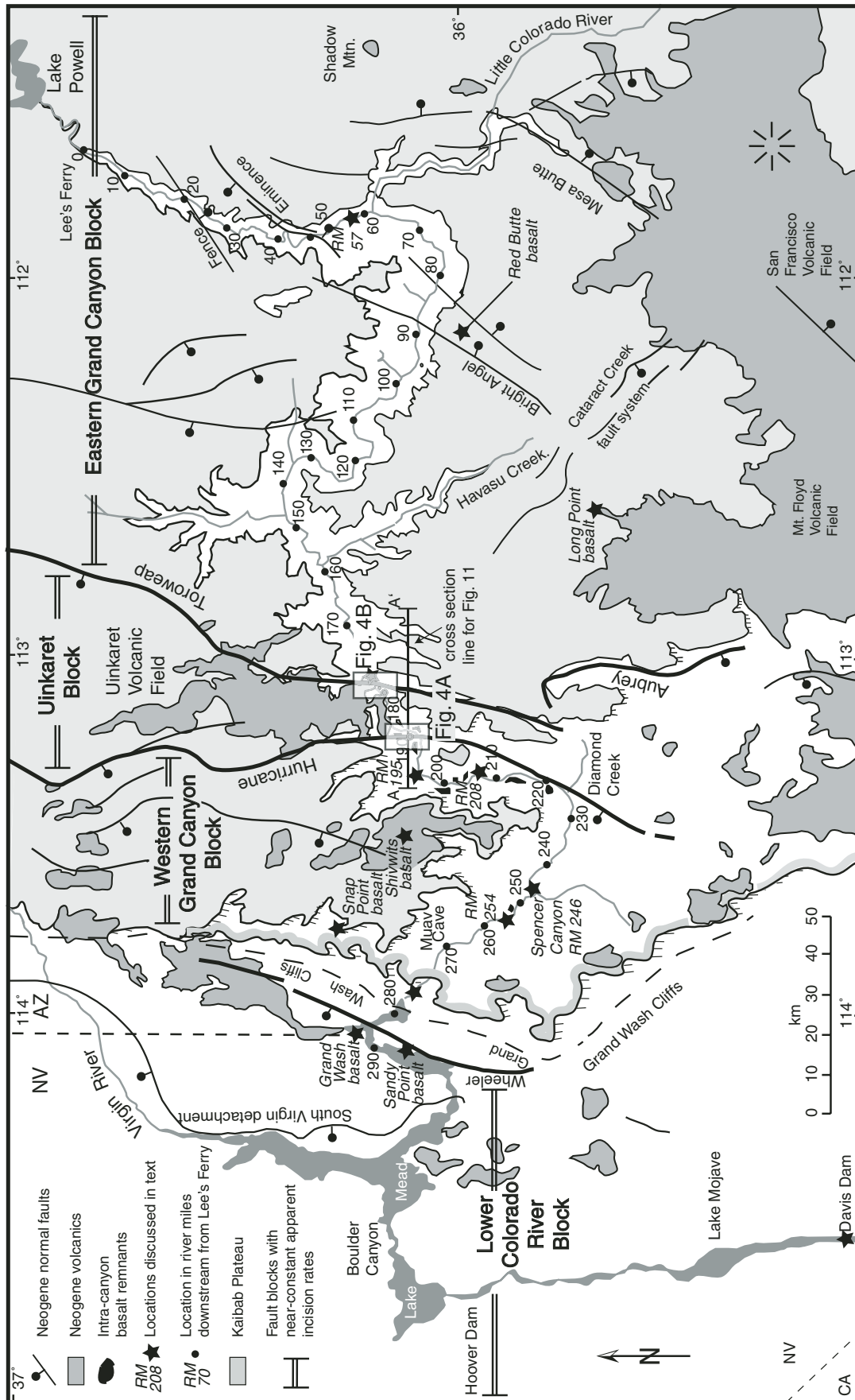
Figure 1. Index map of Grand Canyon region. Dark gray—Quaternary and Tertiary volcanic fields; the Uinkaret volcanic field is bounded by the Toroweap and Hurricane faults. Quaternary intra-canyon flow remnants from the Uinkaret field are preserved in the river corridor between mile 177 and 254 (river miles below Lees Ferry are marked every 10 miles). Areas of detailed maps of flow remnants (boxes) are shown along the Toroweap (Fig. 4A) and Hurricane faults (Fig. 4B). Important locations not on Figure 4 that are discussed in the text are starred.
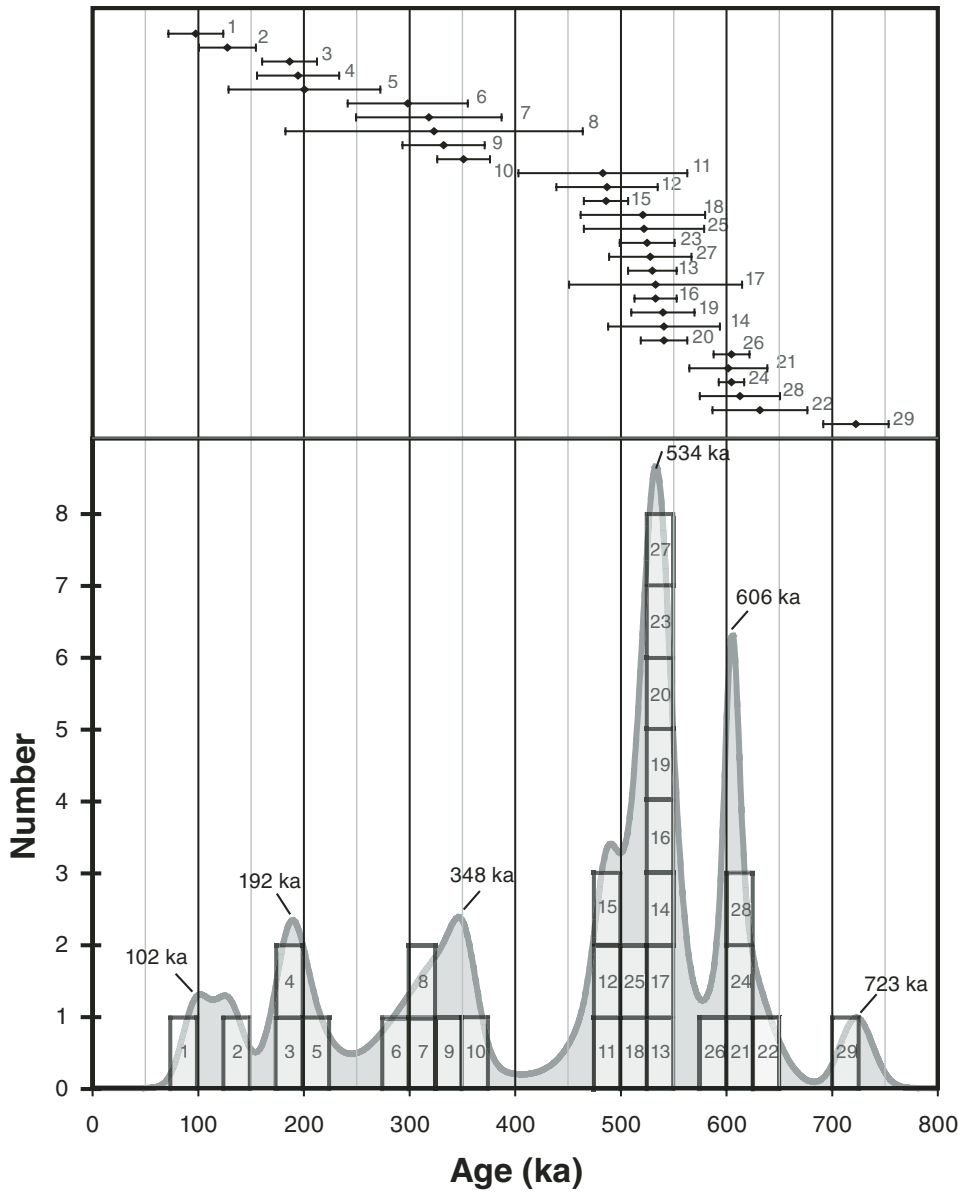
Figure 2. Histogram and age-probability chart of ^{40}Ar-^{39}Ar ages in western Grand Canyon. Numbers correspond to samples listed in Table 1.
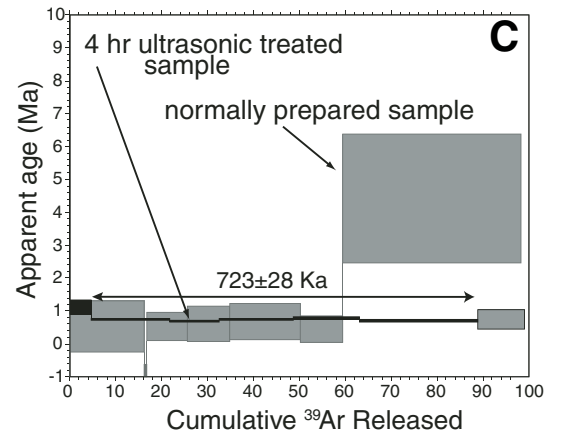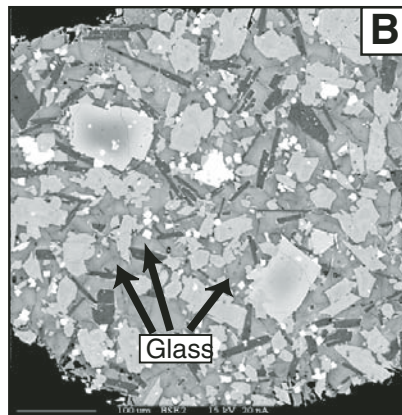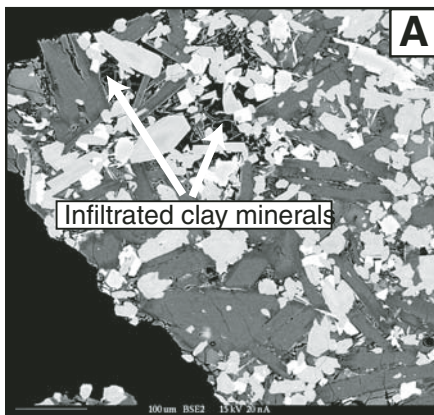

Figure 3. Backscattered electron images (field of view ~500 microns) of Grand Canyon basalt samples containing: (A) infiltrated clay and (B) matrix glass. (C) Age spectra for clay-rich sample improved dramatically with extended ultrasonic treatment.

Figure 4. Maps of flow remnants (modified from Hamblin, 1994 and Huntoon et al., 1981), locations of new dated samples, and age estimates for undated remnants. (A) Toroweap fault and Vulcan's Throne area. (B) Hurricane fault and Whitmore Canyon area. See Figure 1 for map locations.

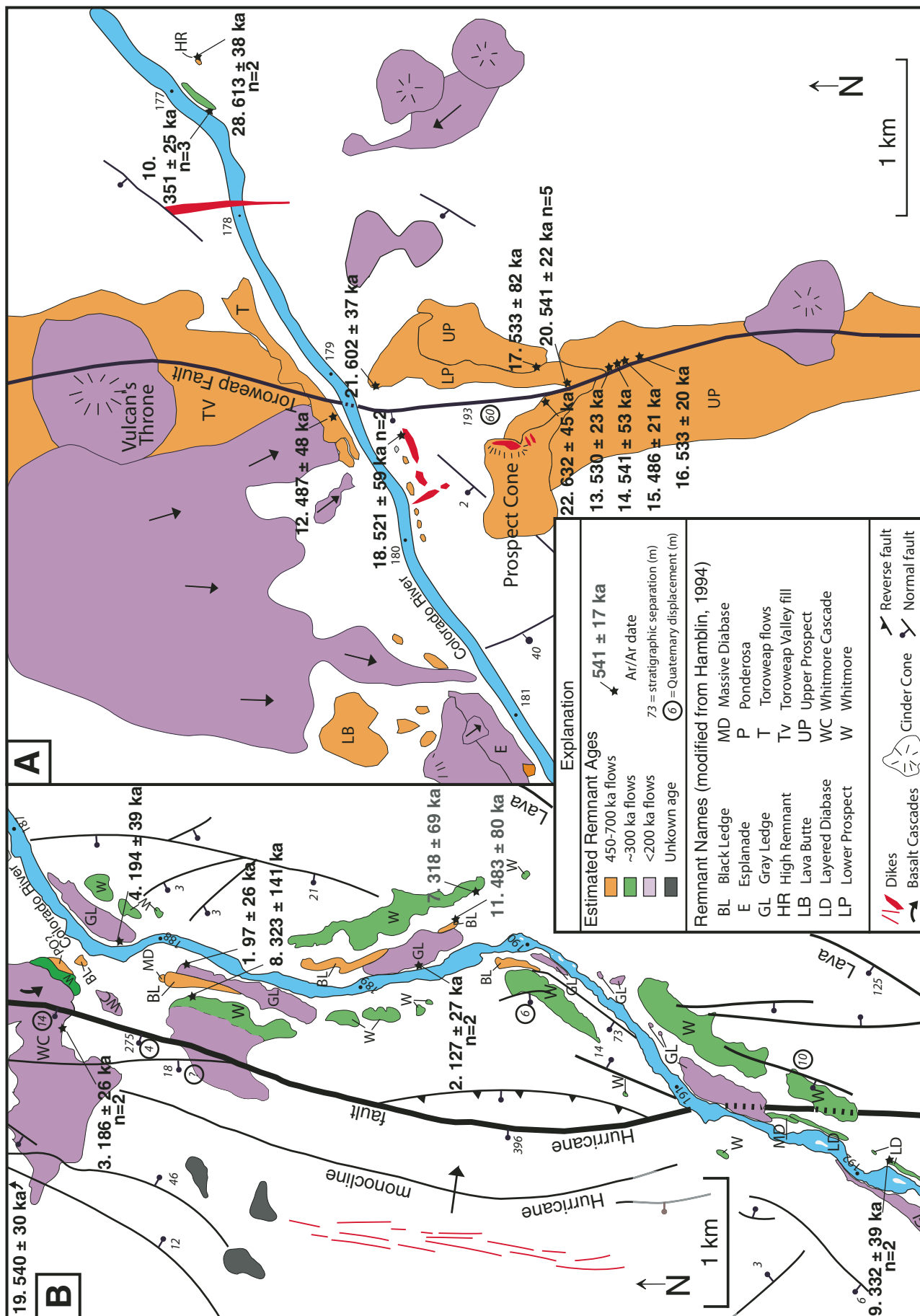TABLE 1. ⁴⁰Ar/³⁹Ar DATES ON BASALTS FROM WESTERN GRAND CANYON

Plotted ages	Basalt flow	Sample number	River mile	Ar/Ar age (ka)	References	Comments
1	Upper Gray Ledge	Mean of two samples	188-189	111 ± 30 *n* = 2	This study	
	Upper Gray Ledge	W00-188-03	188.1R	97 ± 26	Pederson et al., 2002	
2 *n* = 2	Upper Gray Ledge	LP01-189-01 mean of two analyses	189.1L	127 ± 27 *n* = 2	This study	
		LP01-189-01a	189.1L	113 ± 29	This study	
		LP01-189-01b	189.1L	140 ± 29	This study	Longer ultrasonic cleaning
3 *n* = 2	Whitmore Cascade	Mean of two samples	187.6R	186 ± 26 *n* = 2	Raucci, 2004	
		Colonade 1	187.6R	191 ± 30	Raucci, 2004	Float blocks of large columns collected in Whitmore Canyon
		Colonade 2	187.6R	171 ± 50	Raucci, 2004	
	Lower Gray Ledge	Mean of two samples	184-188	195 ± 34 *n* = 2	This study	
4	Lower Gray Ledge	W00-188-02	187.7L	194 ± 39	Pederson et al., 2002	
5	Lower Gray Ledge	LP01-184-01	184.6L	200 ± 72	This study	Longer ultrasonic cleaning, Black Ledge of Hamblin, 1994
6	Massive diabase	W00-195-01	194.8R	298 ± 57	Pederson et al., 2002	
	Whitmore	Mean of two samples	188-190	319 ± 62 *n* = 2	Pederson et al., 2002	
7	Whitmore	W00-190-02	189.6R	318 ± 69	Pederson et al., 2002	
8	Whitmore	LP01-188-01	188.2R	323 ± 141	This study	
9 *n* = 2	Layered diabase	LP01-192-01 mean of two analyses	192.0L	332 ± 39 *n* = 2	This study	
		LP01-192-01a	192.0L	309 ± 20	This study	Longer ultrasonic cleaning
		LP01-192-01b	192.0L	348 ± 17	This study	
10 *n* = 3	Mile 177L	W00-177-02 mean of three analyses	177.3L	351 ± 25 *n* = 3	This study	Pillow basalt blocks intermixed with river sand and gravel
		W00-177-02a	177.3L	349 ± 29	Pederson et al., 2002	
		W00-177-02b	177.3L	385 ± 47	This study	
		W00-177-02c	177.3L	334 ± 36	this study	
11	Black Ledge	Sample from Fenton et al., 2004	189.5L	483 ± 80	Fenton et al., 2004	
12	Toroweap	LP01-179-04	179.1R	487 ± 48	This study	Toroweap C flow
	Upper Prospect	Mean of five samples	179.6L	518 ± 22 *n* = 5	Pederson et al., 2002	
13	Upper Prospect	K00-179-PR3	179.6L	530 ± 23	Pederson et al., 2002	
14	Upper Prospect	K00-179-PR4	179.6L	541 ± 53	Pederson et al., 2002	Upper Prospect flows are listed in stratigraphic order, indicating that the age for #15 seems incorrect, despite its analytical precision
15	Upper Prospect	K00-179-PR5	179.6L	486 ± 21	Pederson et al., 2002	
16	Upper Prospect	K00-179-PR10	179.6L	533 ± 20	Pederson et al., 2002	
17	Upper Prospect	K00-179-PR6	179.4L	533 ± 82	Pederson et al., 2002	
18 *n* = 2	Prospect dike	LP01-179-12 mean of two analyses	179.4L	521 ± 59 *n* = 2	This study	
	Prospect dike	LP01-179-12a	179.4L	498 ± 28	This study	
	Prospect dike	LP01-179-12b	179.4L	559 ± 36	This study	
19	Older Whitmore	WC0424-01	187.2R	540 ± 30	Raucci, 2004	
	Lower Prospect	Mean of three samples	179.6L	568 ± 52 *n* = 3	This study	
20 *n* = 5	Lower Prospect	LP01-179-07 mean of five analyses	179.6L	541 ± 22 n = 5	This study	Upthrown side of fault
	Lower Prospect	LP01-179-07a	179.6L	580 ± 79	This study	
	Lower Prospect	LP01-179-07b	179.6L	527 ± 39	This study	
	Lower Prospect	LP01-179-07c	179.6L	541 ± 28	This study	
	Lower Prospect	LP01-179-07d	179.6L	528 ± 31	This study	
	Lower Prospect	LP01-179-07e	179.6L	608 ± 66	This study	

(continued)

TABLE 1. ^{40}Ar/^{39}Ar DATES ON BASALTS FROM WESTERN GRAND CANYON (*continued*)

Plotted ages	Basalt flow	Sample number	River mile	Ar/Ar age (ka)	References	Comments
21	Lower Prospect	LP01-179-08	179.2L	602 ± 37	This study	D—Dam of Hamblin, 1994
22	Lower Prospect	LP01-179-06	179.6L	632 ± 45	This study	Downthrown side of fault
	Black Ledge	Mean of nine analyses (eight samples)	207-208	572 ± 31 n = 9	Lucchitta et al., 2000	
23	Black Ledge	GC-29-93	207.5L	525 ± 26	Lucchitta et al., 2000	
24 n = 2	Black Ledge	Mean of next two samples	207.5L	605 ± 12 n = 2	Lucchitta et al., 2000	
	Black Ledge	GC-26-93	207.5L	604 ± 16	Lucchitta et al., 2000	
	Black Ledge	GC-26b-93	207.5L	607 ± 18	Lucchitta et al., 2000	
25 n = 2	Black Ledge	Mean of next two samples	207.7L	522 ± 57 n = 2	Lucchitta et al., 2000	
	Black Ledge	GC-34-93	207.7L	559 ± 18	Lucchitta et al., 2000	
	Black Ledge	GC-35-93	207.7L	500 ± 14	Lucchitta et al., 2000	
26 n = 2	Black Ledge	Mean of next two samples	208-209	605 ± 17 n = 2	Lucchitta et al., 2000	
	Black Ledge	GC-24-93	208.2R	609 ± 12	Lucchitta et al., 2000	
	Black Ledge	GC-22-93	208.6R	585 ± 28	Lucchitta et al., 2000	
27 n = 2	Black Ledge	LP01-208-01 mean of two analyses	208.3R	528 ± 39 n = 2	This study	
	Black Ledge	LP01-208-01a	208.3R	525 ± 49	Pederson et al., 2002 (location modified)	
	Black Ledge	LP01-208-01b	208.3R	534 ± 64	This study	Longer ultrasonic cleaning
28 n = 2	176.9-high remnant	Mean of two samples	176.9L	613 ± 38 n = 2	This study	
		K01-177-01	176.9L	643 ± 54	This study	
		K01-177-05	176.9L	601 ± 35	This study	
29	Spencer Canyon	K01-246-01	246.0R	723 ± 31	This study	Black Ledge of Hamblin, 1994
30	Sandy Point basalt	JF-97-76	~290	4410 ± 30	Faulds et al., 2001	Sandy Point basalt

environments. Samples were selected for analysis based on minimal glass, alteration, and clay. Microprobe evaluation included backscattered electron imaging to investigate degree of crystallinity and alteration, potassium distribution within the sample, and quantitative geochemical analysis of a range of phases. We also developed acid leaching and ultrasonic treatments that were effective in removing clay, thereby improving precision and, in some cases, reducing the apparent age of samples (Fig. 3C; Table DR1).

The ^{40}Ar/^{39}Ar ages reported here are weighted-mean plateau ages for the flat central portions of age spectra (Fig. 5). Isochrons for these flat portions generally have atmospheric intercepts and have isochron ages statistically indistinguishable from plateau values. Many of the age spectra have elevated ages at high and/or low temperatures (Fig. 5), attributed to extraneous ^{40}Ar, either as inherited ^{40}Ar in infiltrated clay or within incompletely degassed xenocrysts, or as excess ^{40}Ar in phenocrysts (Fig. 3). All of the ^{40}Ar/^{39}Ar ages are less than 723 ka, and all studied flows have normal paleomagnetic polarity (Hamblin, 1994), consistent with their eruption within the Gauss normal polarity chron (780 ka to present). Thus, complex mechanisms

of post-eruptive reheating previously proposed to explain the normal polarity of flows with ^{40}K/^{40}Ar ages >780 ka are no longer required (cf. Hamblin, 1994). Note that ^{40}Ar/^{39}Ar ages reported here are slightly older (0.6%) than those reported in Pederson et al. (2002b) and Fenton et al. (2004) because ages have been recalculated using the calibration of Renne et al. (1998; Fish Canyon Tuff sanidine age = 28.02 Ma).

Quaternary (<1 Ma) basalts are difficult to date in general, and Grand Canyon basalts have been more difficult than many in the Southwest, in part due to their interaction with river water and clays. Although these dates are dramatically better than older ^{40}K/^{40}Ar dates, there are relatively large uncertainties in age measurements, both in terms of precision and accuracy. Two sigma analytical precision is typically ±5%–30% (Table 1), but the quoted precision associated with individual analyses may not adequately reflect the accuracy of the measurements. For example, the two analyses of sample 9 yielded ages of 309 ± 20 and 348 ± 17, but the ages do not overlap within the calculated 2 sigma error. There are also a few instances where the geologic context shows that the accuracy of ages is not reflected in the reported precision. For

example, samples 13–17 were sampled in stratigraphic order in a flow stack on Upper Prospect flows in Prospect Canyon (Fig. 5. Four of these ages are in close agreement and indicate that this sequence of flows was likely emplaced rapidly (close to 533 ka), but the 486 ± 21-ka age on sample 15, in spite of its high precision, is incompatible with its stratigraphic position and is outside the 2 sigma precision of its neighbors. For samples like these, with MSWD (Mean Square Weighted Deviate) values >1, we follow the method of Dalrymple and Hamblin (1998) of recalculating errors to better reflect scatter of the dates beyond analytical error.

Another way to evaluate accuracy is to compare multiple analyses from the same sample. In most cases (samples 2, 10, 18, 20, 27, but not 9), the multiple analyses overlap within the reported 2 sigma precision. Also, in most cases, when two or more samples were taken from the same flow (sample 3 and samples 13/14) or flows were believed to be correlative (samples 16 and 17), ages also overlap within 2 sigma precision.

The results are shown in Figure 2. Nineteen of the well-dated samples range in age from 480 to 723 ka, with age-probability peaks at 534, 606, and 723 ka (Fig. 2). These samples come
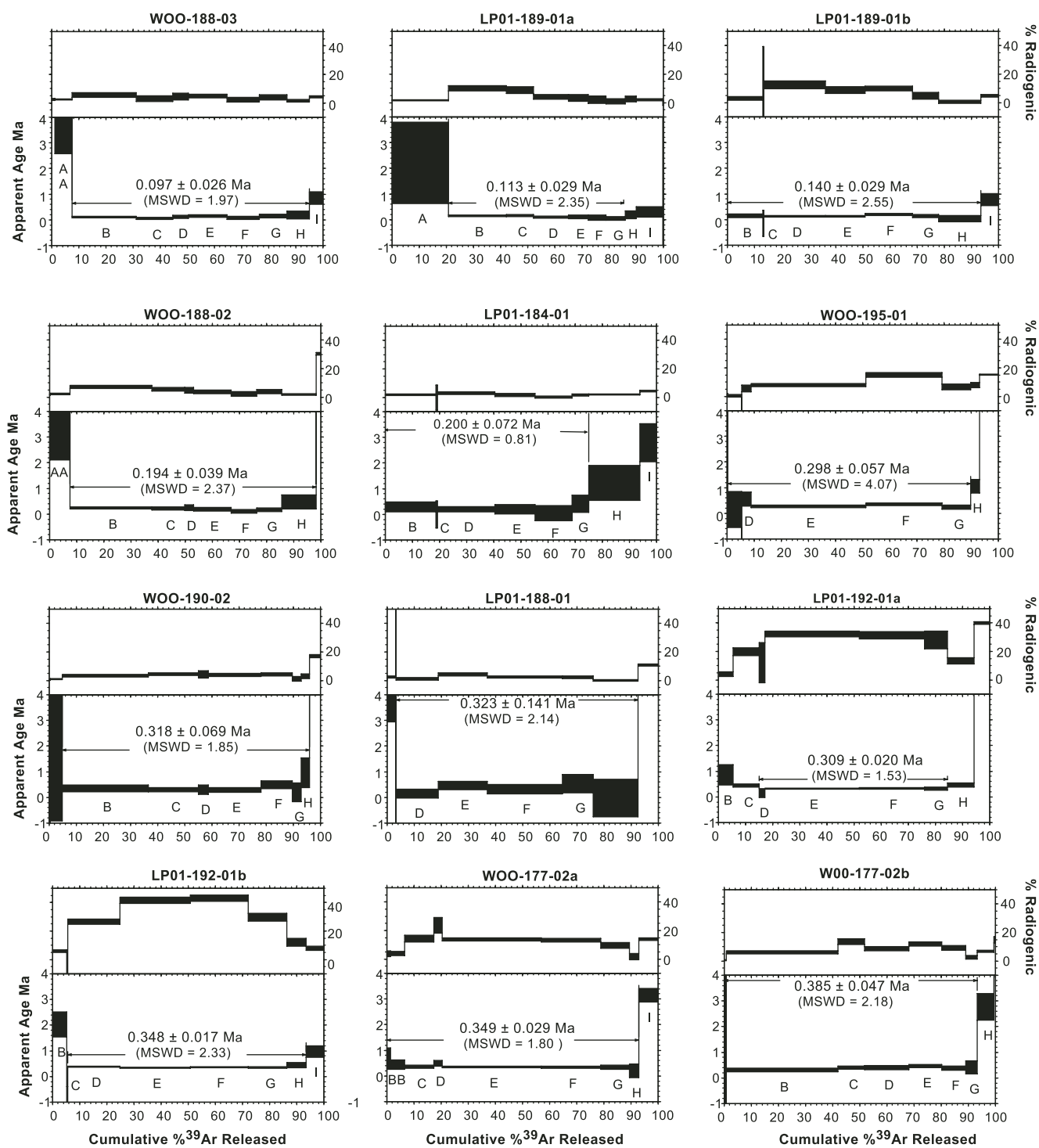
Figure 5. $^{40}Ar/^{39}Ar$ spectra for dated basalt samples. Reported ages are weighted-mean plateau ages for the flat central portions of age spectra. (*Continued on following two pages*.)
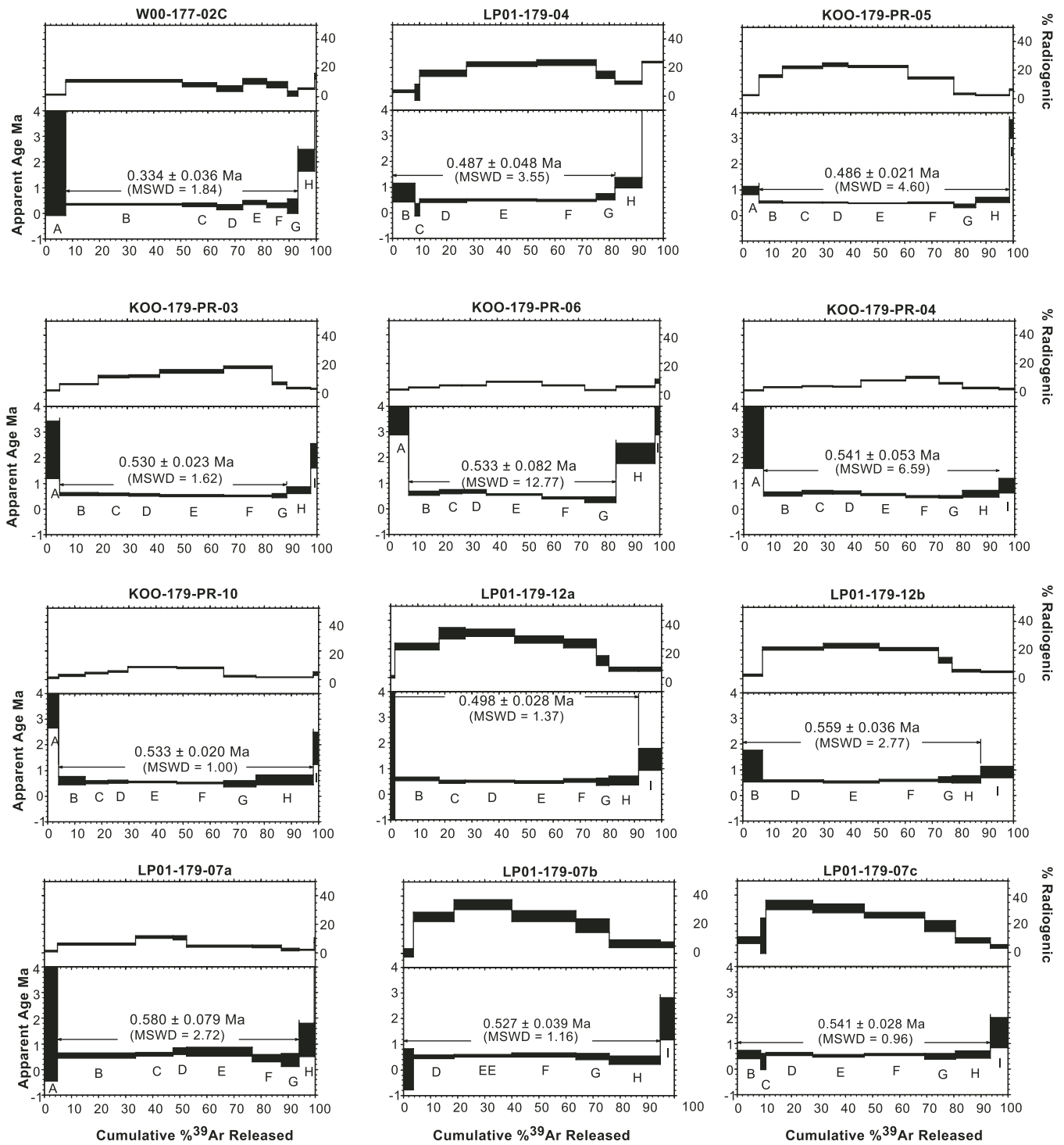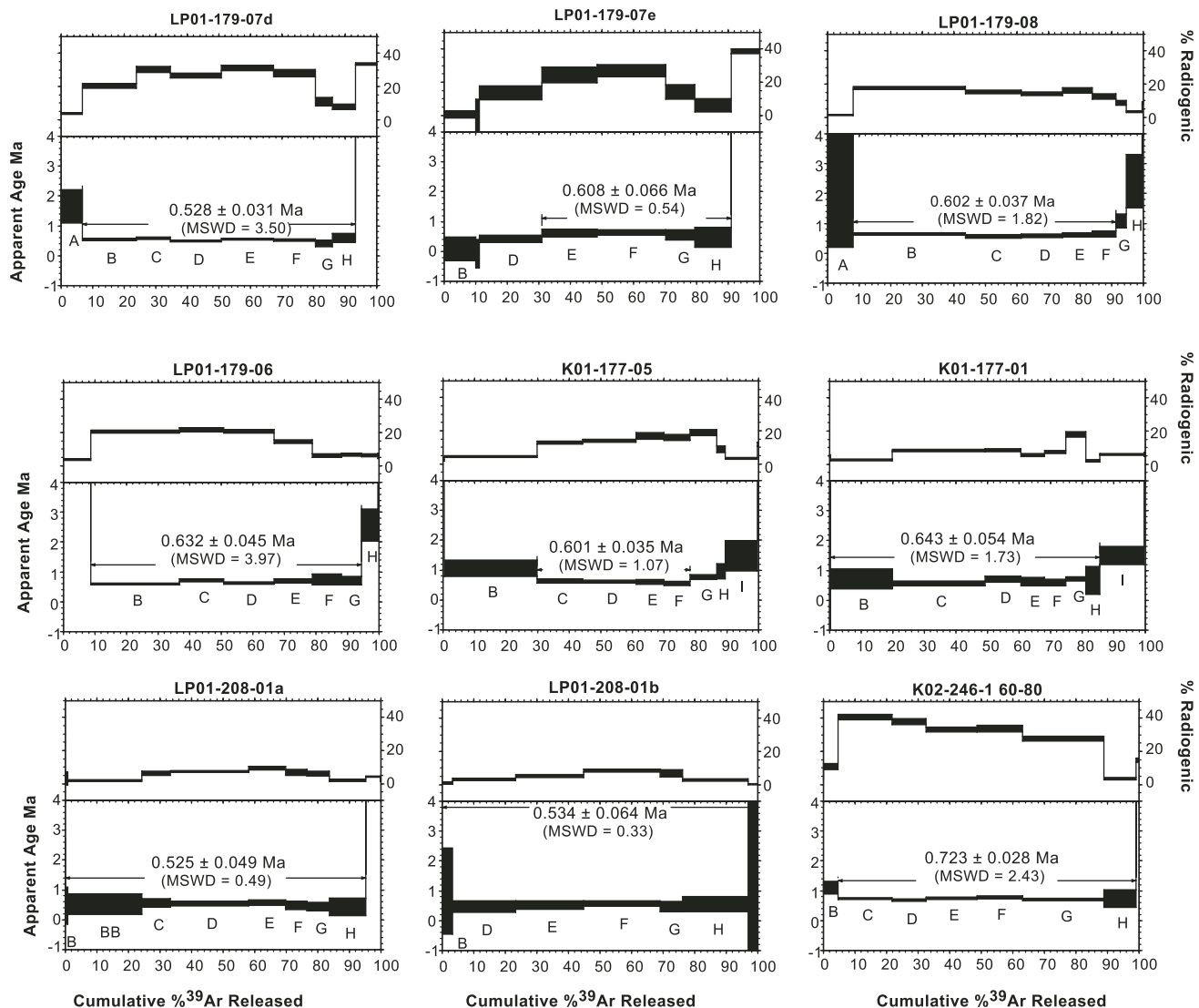
Figure 5 (continued).

Figure 5 (continued).

mainly from flows in the vicinity of the Prospect Canyon/Toroweap fault (Fig. 4A). The oldest $^{40}Ar/^{39}Ar$ age is 723 ± 31 ka (2 sigma error) for a single sample of a >17-m-thick flow remnant at RM 246 at the mouth of Spencer Canyon in western Grand Canyon (Figs. 1 and 6). Based on our correlation of flow remnants, we interpret this flow to have traveled ~110 km down the river from a series of edifices within Grand Canyon and along Toroweap fault (Fig. 4A; Crow et al., 2007).

Basalts ranging in age from 525 to 650 ka include Lower Prospect flows of Prospect Canyon (LP, Fig. 4A), high remnants of basalt upstream of Toroweap fault (HR, Fig. 4A), and flows near RM 208 named Black Ledge (Fig. 1; Hamblin, 1994; Lucchitta et al., 2000). Units ranging in age from 480 to 540 ka include

Upper Prospect flows (UP, Fig. 4A), Prospect Cone dike, Toroweap A flow, and Black Ledge remnants near RM 189.5 (Fig. 4B) and at Granite Park near RM 208. Numerous dated Black Ledge flows at Granite Park come from four separate outcrop remnants (both sides of the river) that are likely correlative flows. We were unable to match the high precision reported by Lucchitta et al. (2000). Multiple-age flows may indeed be present (Lucchitta et al., 2000), but existing ages are not decipherable in terms of just two ages of flows.

There is abundant field evidence for multiple flows in the 480- to 723-ka age range, accumulating to thicknesses of >500 m in proximal areas (Prospect Canyon) and also present as superposed flows in distal areas (Granite Park). The farthest-traveled flow in Grand Canyon

(RM 254) is undated, but is assumed to be in this age range. A single 540 ± 30 ka dated basalt ~3 km northwest of the Colorado River at RM188 (Fig. 4B) erupted from a cinder cone near the Hurricane fault (Raucci, 2004) and demonstrates that there was also volcanism elsewhere in the Uinkaret Volcanic field in this interval. It is tempting to designate the 534- and 606-ka peaks (Fig. 2) as Lower and Upper Prospect flows, respectively, and correlate them with two different age flows at Granite Park, but this remains unproven. Thus, pending additional dating of geologically well constrained samples, we view the multiple peaks at 534, 606, and 723 ka in the age-probability plot (Fig. 2) to be part of a broad time span of 480- to 723-ka volcanism, but not necessarily an accurate representation of discrete flow events.

A younger set of flows has a range in age from 298 to 325 ka and an age probability peak of 348 ka (Fig. 2). These flows include the Whitmore flow (W, Fig. 4B), Layered Diabase (RM 192, Fig. 4B), Massive Diabase (RM 195, Fig. 1), and the 177-mile basalt that flowed upstream to its present location (Fig. 4A; Crow et al., 2007). The largest volume of 300- to 350- ka basalt was erupted along the Hurricane fault in the area of Whitmore Canyon.

The youngest flows we have dated are 100- to 200- ka flows near Whitmore Canyon. Age probability peaks are at 192 and 102 ka (Fig. 2). The "Gray Ledge" flow of Hamblin (1994) has a lower (ca. 200-ka) and upper (ca. 100-ka) component. Upper Gray Ledge flows at river mile 188.1 and 189.1 are 97 ± 26 and 127 ± 21 ka, respectively. A lower Gray Ledge (mile 187.7) and one flow previously referred to as "Black Ledge" (mile 184.7, now identified as lower Gray Ledge) give ages of 194 ± 39 and 200 ± 72 ka, respectively (Table 1).

Methods of Calculating Bedrock Incision Rates

The new basalt ages allow us to calculate incision rates in numerous places in western Grand Canyon. The Colorado River system in Grand Canyon preserves a series of inset Quaternary alluvial terraces at various heights that record climatically controlled aggradation and incision episodes superimposed on a history of overall exhumation and deepening of the bedrock canyon (Pederson et al., 2002b, 2006; Anders et al., 2005). Methods for calculating incision rates are refined from those of Pederson et al. (2002b) and need elaboration to help evaluate the variable quality of incision data points. Basalt flows locally rest on top of river gravels that overlie bedrock straths within the river corridor, near the modern river channel (Figs. 4 and 7). The straths represent times of erosion of the bedrock channel by the river (Bull, 1991) and hence times of canyon deepening. Dates obtained from materials directly above the straths, such as basalt flows or travertine, thus provide a close approximation of the time of formation of the strath (Pederson et al., 2002b; Pazzaglia et al., 1998). Height of the strath above the 10,000 cubic feet per second (283 m³/s) reference river level was measured with a Jacob staff and/or estimated from LIDAR (Light Detection and Ranging) measurements of height of the base of flows. Straths are interpreted as a past position of part of the bedrock river channel before emplacement of the basalt or other dated material.

Our first method of estimating bedrock incision is to compare the height of the strath relative
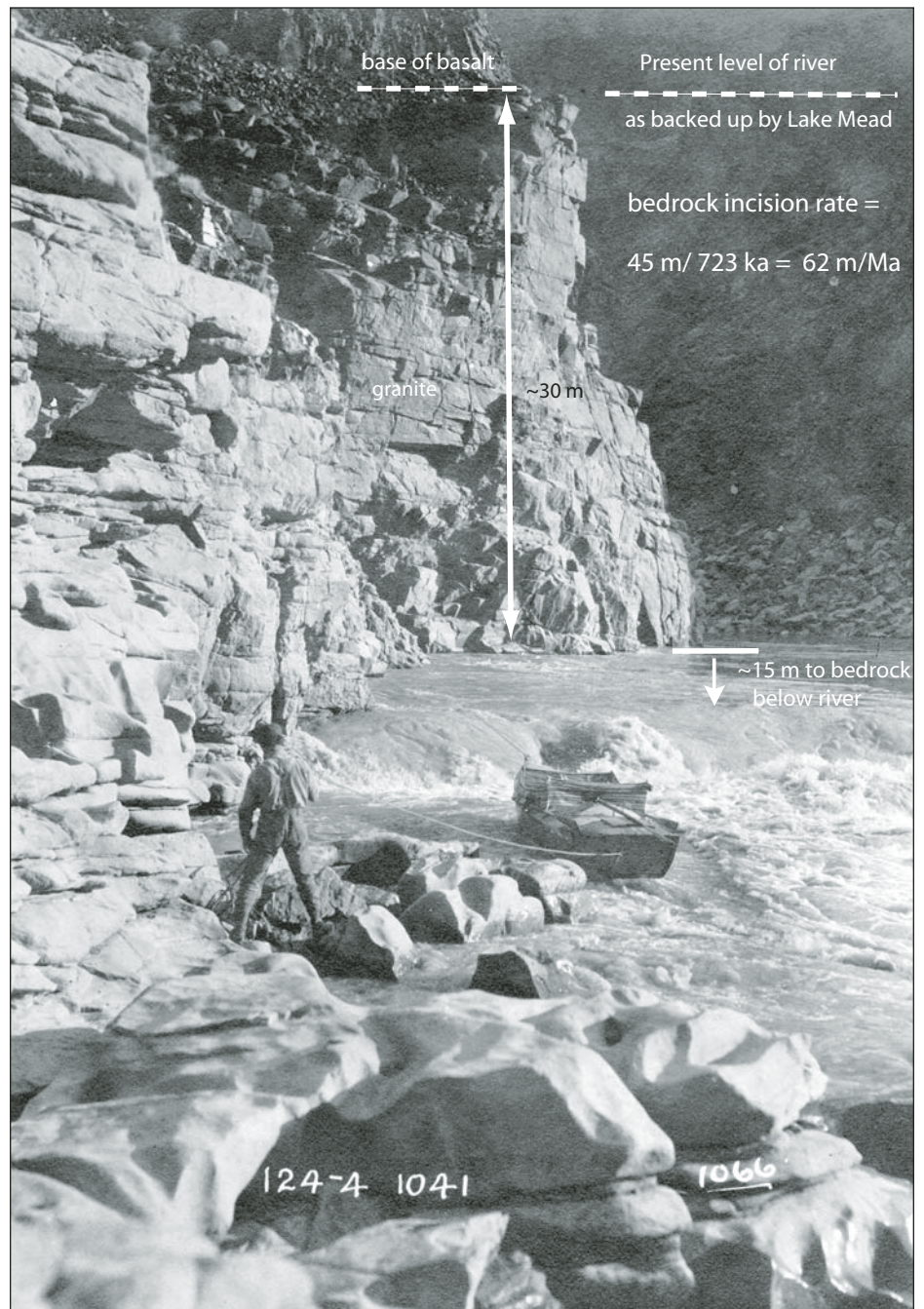

Figure 6. Photo of Lava Cliff Rapids (RM 246) showing base of 723-ka basalt remnant and its ~30-m pre-dam height above the river. Maximum depth to bedrock of 15 m was determined by drilling at Bridge Canyon Dam site ~8 river miles (13 km) upstream, suggesting a bedrock incision rate of 62 m/Ma. Northern Arizona University, Cline Library, Special Collections and Archives, Julius F. Stone collection.

to the inferred position of the bedrock surface beneath the modern river (method A in Fig. 6). Our preferred estimate of depth to bedrock under the river is the "maximum pool depth," defined as the mean of the ten deepest pools for a 15-mile-long reach centered on the dated remnant.

These values are calculated using bathymetry data that were generated using sonar (Wilson, 1986). This method uses slightly deeper bedrock depths than Pederson et al. (2002b), and provides systematic estimates of bedrock incision and deepening of Grand Canyon.
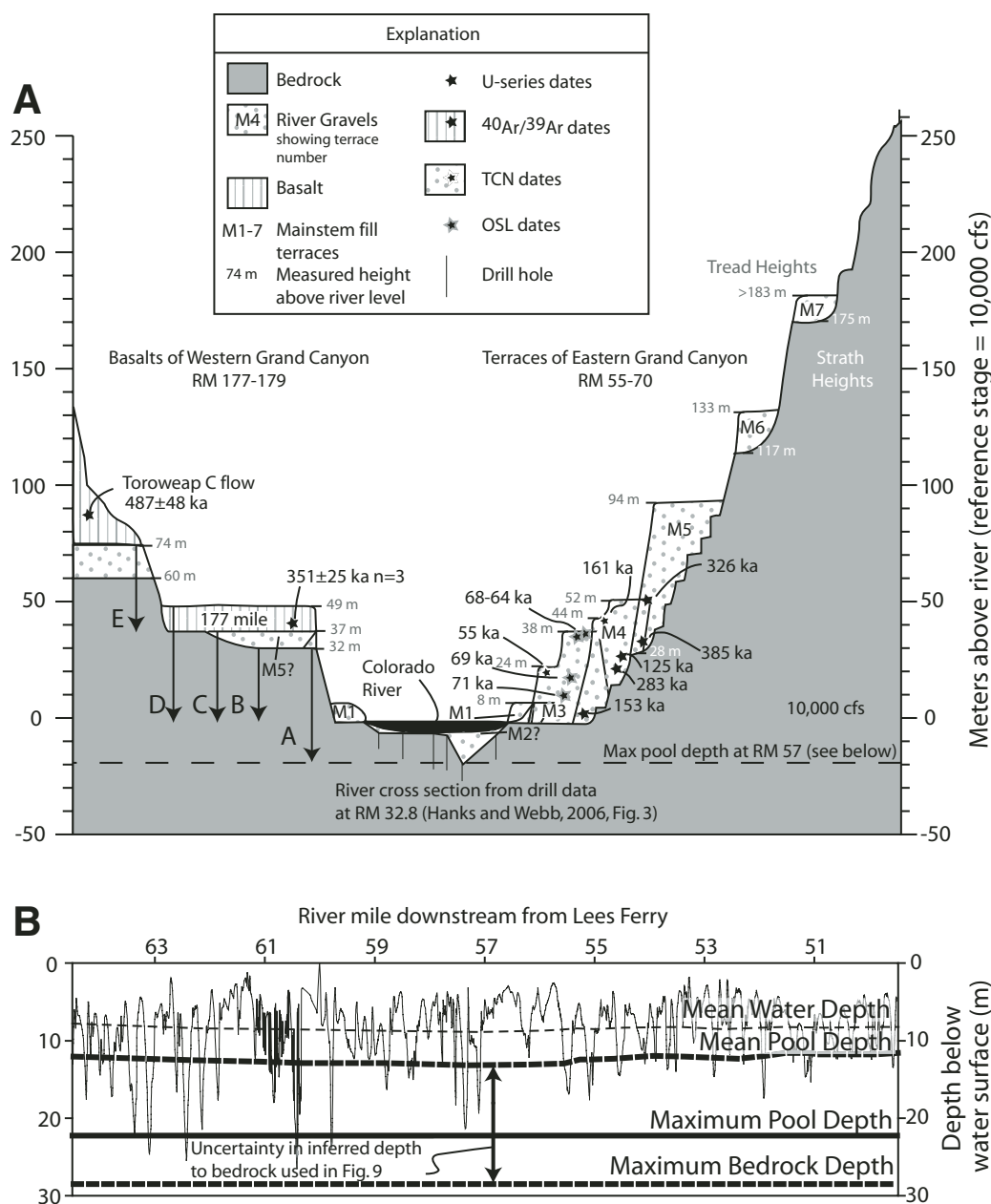
Figure 7. (A) Schematic summary of Grand Canyon terraces, strath and tread heights, and geochronology. The right side shows U-series dates on terrace fills from eastern Grand Canyon (from Anders et al., 2005; Pederson et al., 2006); left side shows Ar-Ar basalt dates from western Grand Canyon (this paper). Methods for calculating incision amounts based on dated samples are shown at lower left: A—from bedrock strath to inferred depth of bedrock below river level based on pool depths (Pederson et al., 2002b and this paper); B—from bedrock straths to 10,000 ft³/s (283 m³/s) river level; C—from height of dated sample to river; D—from top of aggradational terrace or basalt flow to present river level (Lucchitta et al., 2000); E—from strath to strath height differences in a given reach plus an understanding of duration of fill events (Pederson et al., 2006 and this paper). An example of lateral variation of depth to bedrock beneath the river is shown based on drill data at RM 32.9 (Hanks and Webb, 2006). (B) Example of bathymetry data (Wilson, 1986), showing mean water depth, mean pool depth, maximum pool depth, and maximum bedrock depth used in Figure 9 to infer uncertainty in depth to bedrock.

There are inherent geologic uncertainties in our bedrock incision calculations that also apply to other bedrock incision studies (e.g., Merritts et al., 1994; Burbank et al., 1996; Pazzaglia and Brandon, 2001). The first uncertainty is that the dated material provides only a minimum age of the strath, with unknown hiatus between beveling of the strath, deposition of river gravels, and deposition of the dated material. In this regard, our quoted rates may be maximum bedrock incision rates.

A second and probably larger uncertainty is that the mean depth to bedrock beneath the present river remains poorly known. Bathymetric data (Figs. 7 and 8) suggest that the river channel, like the river banks at lowest flows and like most side-stream tributaries, is highly pot-holed and is floored by a mixture of bedrock and alluvial fill. The resulting modern bedrock "strath" is highly nonplanar both laterally (Fig. 7, river cross section from Hanks and Webb, 2006) and longitudinally (Fig. 8). For incision calculations, we define "pools" as areas where water depths are greater than the mean water depth. Mean pool depth in Grand Canyon is 9–17 m; maximum pool depth (mean of the ten deepest pools in a 15-mile-long reach) is 19–24 m, and *maximum* depth to bedrock based on drilling and seismic studies is ~28 m (Fig. 8).

A third uncertainty is that some basalt remnants may have flowed onto alluvial terraces resting on elevated bedrock benches rather than into the paleothalwag. In this regard, our rates may tend to be maximum bedrock incision rates.

We portray the geologic uncertainty in depth to bedrock in our incision vectors (Fig. 9) by showing mean pool depth (which gives the minimum bedrock depth/minimum incision rate), maximum pool depth (preferred bedrock depth/preferred incision rate), and maximum bedrock depth (maximum incision rate). The 2-sigma analytical precision of the age analysis is used in the same way as previous workers (Fenton et al., 2001; Pederson et al., 2002b). The combined
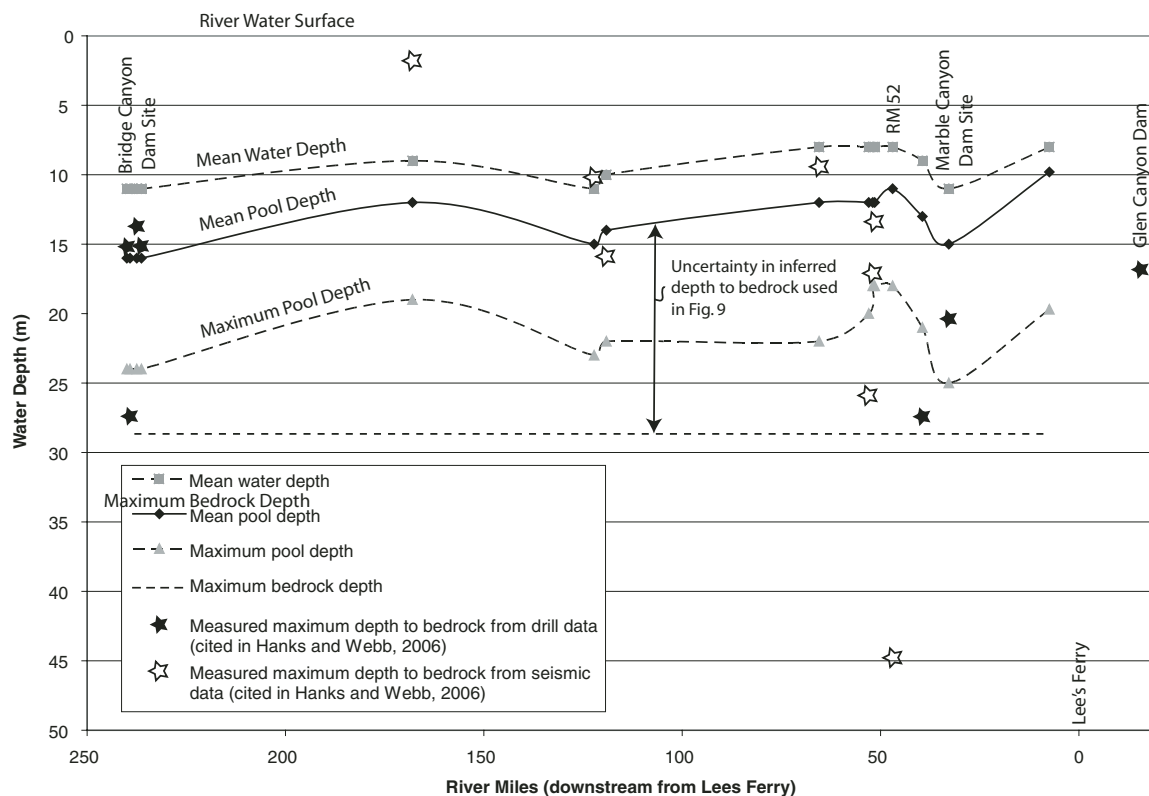
Figure 8. Bathymetry, mean water depth, mean pool depth, maximum pool depth, and measured maximum depth to bedrock in the Colorado River of Grand Canyon. Bathymetry from Wilson (1986) from Lees Ferry to RM 235 based on sonar studies (no data below RM 235 where river bottom has been silted in by Lake Mead). Measured maximum depth to bedrock (from Hanks and Webb, 2006) is based on drilling done to evaluate dam sites and seismic studies of river banks. Maximum pool depth is used in this paper as the best proxy for mean depth to bedrock.

estimates of both geologic and analytical uncertainties (Fig. 9) show that the large and systematic incision-rate variations between eastern and western Grand Canyon that lead to the main conclusions of this paper are robust.

A second method for estimating bedrock incision rates is to compare the ages of straths of different heights in the same reach (Pederson et al., 2006). This method provides an estimate of bedrock incision that is independent of depth to bedrock and also allows data from fill terraces to be considered. This analysis emphasizes that the times when the Colorado River was incising bedrock may have been relatively short, less than half of its Quaternary history, and that the rest of the time it is aggrading its bed and, hence, not incising the canyon. Using this method, Pederson et al. (2006) reported an average incision rate of ~142 m/Ma in eastern Grand Canyon for the last 385 ka. Addition of new data points from this study refines this estimate to apparent rates of 172 m/Ma in eastern Grand Canyon and 55 m/Ma in western Grand Canyon (Fig. 10). By projecting the regressed lines through our best incision points to below

river level (Fig. 10), this method suggests that average depth to bedrock in the eastern Grand Canyon is 28 m (in agreement with the deepest measurements found so far from drilling; Fig. 7), and in the western canyon is 9 m (shallower than the 15-m depths determined from drilling at Bridge Canyon dam site). Additional high-quality incision points, once obtained, will help refine these numbers such that this method shows great promise for estimating both long-term average apparent incision rates and average depth to bedrock in different reaches.

Differential Bedrock Incision Rates

Figure 11 and Table 2 summarize bedrock incision-rate data points from Grand Canyon, most of which are newly reported in this paper. The eastern Grand Canyon rates are uniform from RM 57 (with points 2, 3, 4, and 5 of Table 2 giving a mean incision rate of 150 m/Ma), to RM 177–179 (with points 7 and 8 of Table 2 giving a mean of 155 m/Ma). These rates are somewhat less than the regressed line through the same points (172 m/Ma) because

of depth to bedrock assumptions. The points at RM 177 and 179, just east, and in the immediate footwall, of the Toroweap fault, are based on dated basalt remnants that overly river gravels, with evidence for basalt-water interactions in the form of pillows and sand-filled fractures in the basal basalt. Importantly for this study, the combined fill terrace dates and basalt data (Fig. 10) indicate that there was a uniform average bedrock incision rate for the entire reach of eastern Grand Canyon (RM 56–179) for the time interval 153–487 ka, in spite of aggradation and incision episodes (Fig. 10; Pederson et al., 2006). Basalt data in several other places (e.g., RM 177–179, RM 188, RM 204–208, and RM 246) also suggest a uniform bedrock incision rate within a given reach of Grand Canyon back to 723 ka, as discussed below.

Well-constrained, measured incision rates (Fig. 9; Table 2) change abruptly across the Toroweap fault, to values of 50–70 m/Ma. This is interpreted to indicate that lowering of the western block by faulting results in dampening of the eastern Grand Canyon incision rate to produce a lowered "apparent incision
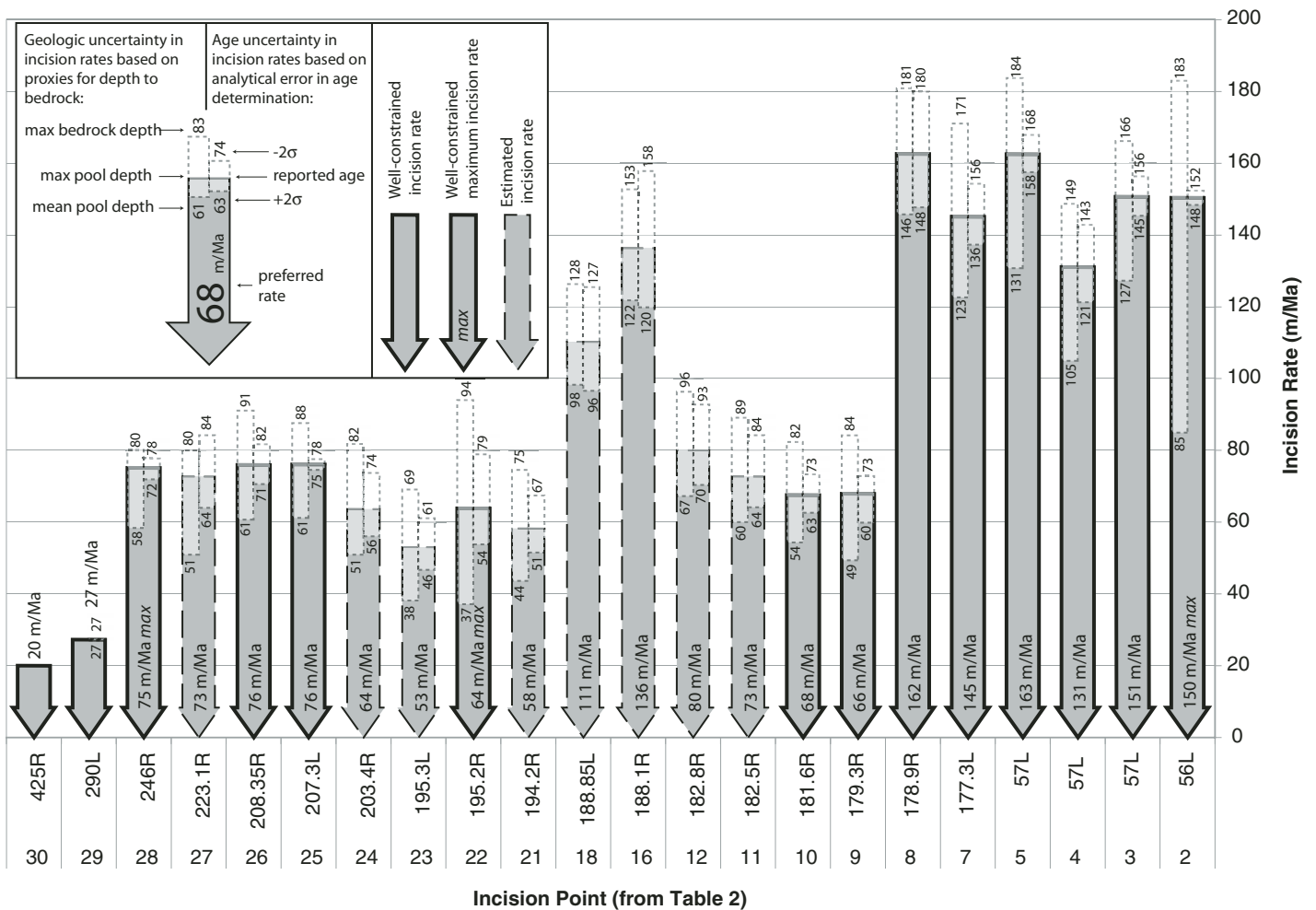
Figure 9. Incision data points from Table 2, arranged by river mile, showing both analytical and geologic uncertainties for incision rates. Gray vector shows preferred incision vectors based on reported age and maximum pool depth. Upper right boxes show incision rate uncertainty based on geochronological uncertainty (± 2σ). Upper left boxes show incision-rate uncertainty based on use of mean pool depth and maximum bedrock depth (from Fig. 8).

rate." Figure 11 shows a systematic variation in apparent incision rates within the Uinkaret block: rates increase progressively westward from the fault and nearly regain the eastern Grand Canyon rate ~6 km west of the Toroweap fault. Immediately west of the Hurricane fault, apparent incision rates diminish again abruptly to 60–70 m/Ma, and remain relatively uniform; they do not again approach the eastern Grand Canyon rates for the entire western Grand Canyon block (to RM 246).

An important new data point is the 723 ± 28-ka remnant exposed opposite the mouth of Spencer Canyon (Fig. 6, RM 246) that flowed ~100 km along the Colorado River bed. The basalt is perched on Precambrian granite directly above the river channel. Although no gravel is exposed at the strath, the remnant is directly opposite a major side canyon (Spencer Canyon) at the head of what used to be Lava

Cliff rapids (now silted in by Lake Mead) and is interpreted to have been emplaced in the paleo-thalwag. The top of this flow is at an elevation of 381 m (based on LIDAR), and the base of the flow, at 350 m, is just exposed above the present lake-controlled river level. This reach of the river has been flooded by Lake Mead, but historic photographs (Fig. 6) as well as pre-dam contour maps and surveyor's descriptions of the Spencer Canyon Power Site (LaRue, 1925, plate LIX) show that the base of the flow was ~30 m above the river level at the head of Lava Cliff rapids (Fig. 6). Dam-site surveyors guessed that bedrock at the dam site would be less than 12 m below river level based on the presence of bedrock outcrops in the rapid (LaRue, 1925, p. 94), in good agreement with the 15-m depth of bedrock near Bridge Canyon dam site (RM 238). Hence, bedrock incision has averaged 58–62 m/Ma since this flow was emplaced (Table 2). In

this case, because of the nearby drill data, the maximum bedrock depth is probably most accurate; nevertheless, using the maximum pool depth method for consistency (Figs. 9 and 11), the incision value increases to 75 m/Ma.

The dashed incision vectors in Figure 11 are less well constrained than the solid ones, but are also considered important data points. The Lava Falls (RM 182.8) and Buried Canyon flows (RM 182.5; Hamblin, 1994) represent basalt flows that completely filled the paleothalwag plugging the river and shifting the river to its present more southerly location. The basal Buried Canyon basalt flow (flow "A" of Hamblin, 1994), the covered base of which is 66 m above river level gives a *maximum* incision rate of 155 m/Ma, if we assume an age of 550 ka, consistent with a correlation to the 475- to 625-ka Prospect and Black Ledge flows, as suggested by LIDAR correlations (Crow et al., 2007). Similarly, at
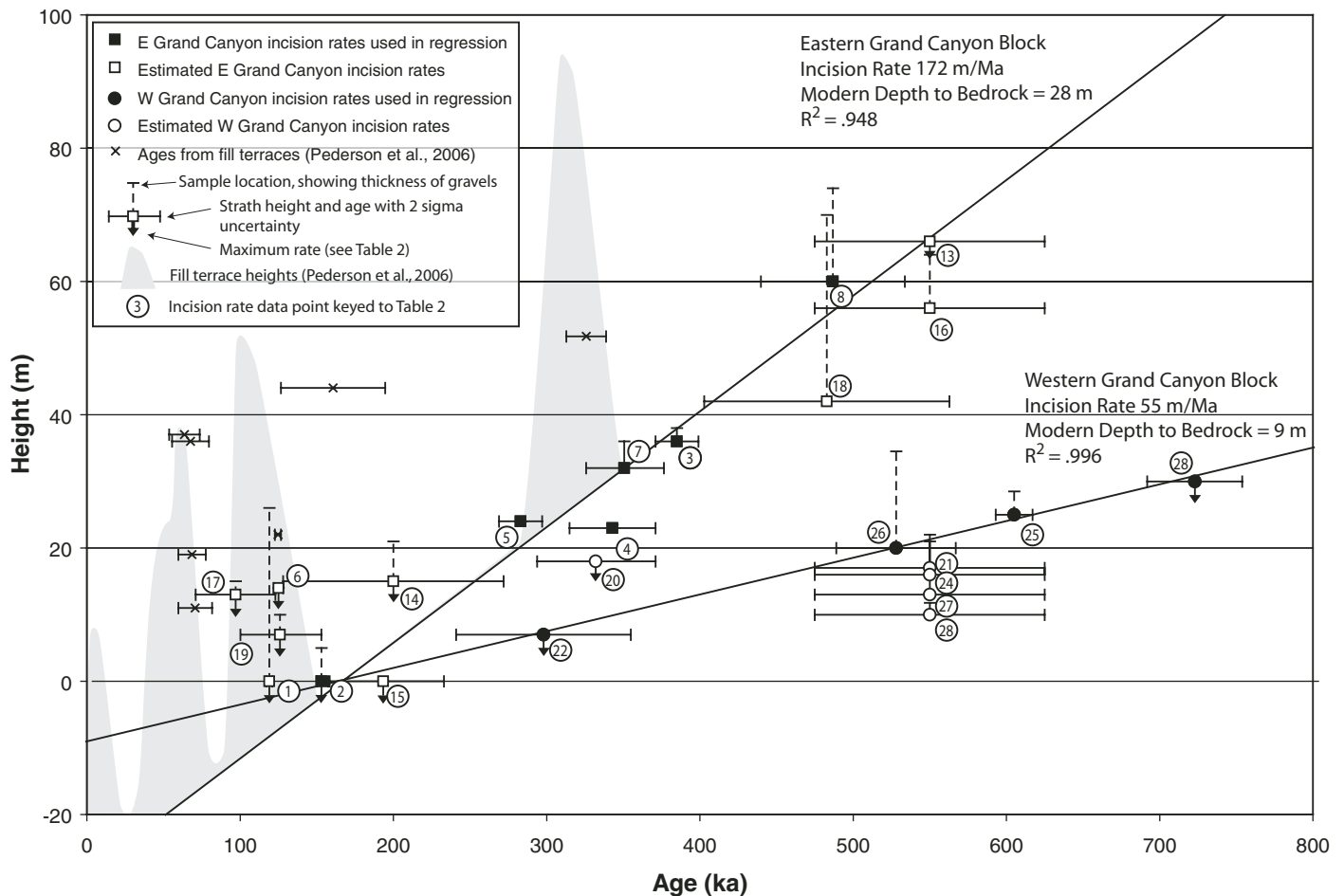
Figure 10. Alternate method of calculating incision rates (modified from Pederson et al., 2006) uses strath to strath heights and ages (data from Table 2) to give average incision rates of 173 m/Ma in the eastern Grand Canyon and 55 m/Ma in western Grand Canyon. Dated fill terraces and heights (light gray) show climatically influenced aggradational and incision intervals (modified from Pederson et al., 2006).

the mouth of Whitmore Wash (RM 188.1), a rate of 136 m/Ma would result, assuming the flow mapped as "Massive Diabase" by Hamblin (1994; see Table 2) correlates instead with the 475- to 625-ka Prospect and Black Ledge flows as suggested by LIDAR heights.

Fault Displacement: Magnitudes and Rates

Toroweap Fault

The Toroweap fault is part of a several hundred-km-long, N-S–striking normal fault system (Hamblin, 1970a), which is part of the distributed system of normal faults that forms the microseismically active neotectonic edge of the Colorado Plateau (Fig. 1; Brumbaugh, 1987). South of Grand Canyon, the Toroweap fault links with the Aubrey fault; north of Grand Canyon, it extends ~250 km as the active Sevier/Toroweap fault zone (Fig. 1; Pearthree et al, 1983; Pearthree,

1998; U.S. Geological Survey and Arizona Geological Survey, 2006). Total west-down stratigraphic separation of Paleozoic units is variable along strike. For the location where it crosses Grand Canyon, stratigraphic separation has been variably reported (177–370 m; Table DR2), but we use the value of 193 m of McKee and Schenk (1942), based on offset of key horizons in the Cambrian part of the section.

Total post-basalt (post–600-ka) slip on the Toroweap fault where it crosses Grand Canyon has been reported as 44 m (McKee and Schenk, 1942), 46 m (Hamblin, 1970a), and 60 m (this paper). Late Quaternary separation is about one-half (Billingsley, 2001) to one-third (this study) of total stratigraphic separation (Table DR2). This has been interpreted to mean that the fault is one of the youngest and most active normal faults in western Grand Canyon (Jackson, 1990), likely less than 2–3 million years old.

The new dates on the Upper Prospect flows in Prospect Canyon (Fig. 4A) and on the Toroweap C flow (Fig. 12C) help refine estimates of displacement rate (Jackson, 1990; Fenton et al., 2001). As shown in Figures 12A and 12B, the contact between the highest Prospect Canyon basalt flow and the base of the Quaternary sidestream fill terraces at the rim of Prospect Canyon basalt is offset a total of 52 m by the fault (three strands). This measurement is comparable to the measurement of 46 m by Huntoon (1977) that was presumably taken on the main strand. Using the 52-m offset (Fig. 12), combined with the 518 ± 22-ka mean age of the Upper Prospect flows, yields a displacement rate of 100 m/Ma. Likewise, a marker red sandstone (Figs. 12A and 12B) just above the lower Prospect flow (mean age of 568 ± 52 ka) is offset 60 m, yielding a slip rate of 106 m/Ma. Figure 12 shows that the new Ar-Ar ages for basalts generally agree with
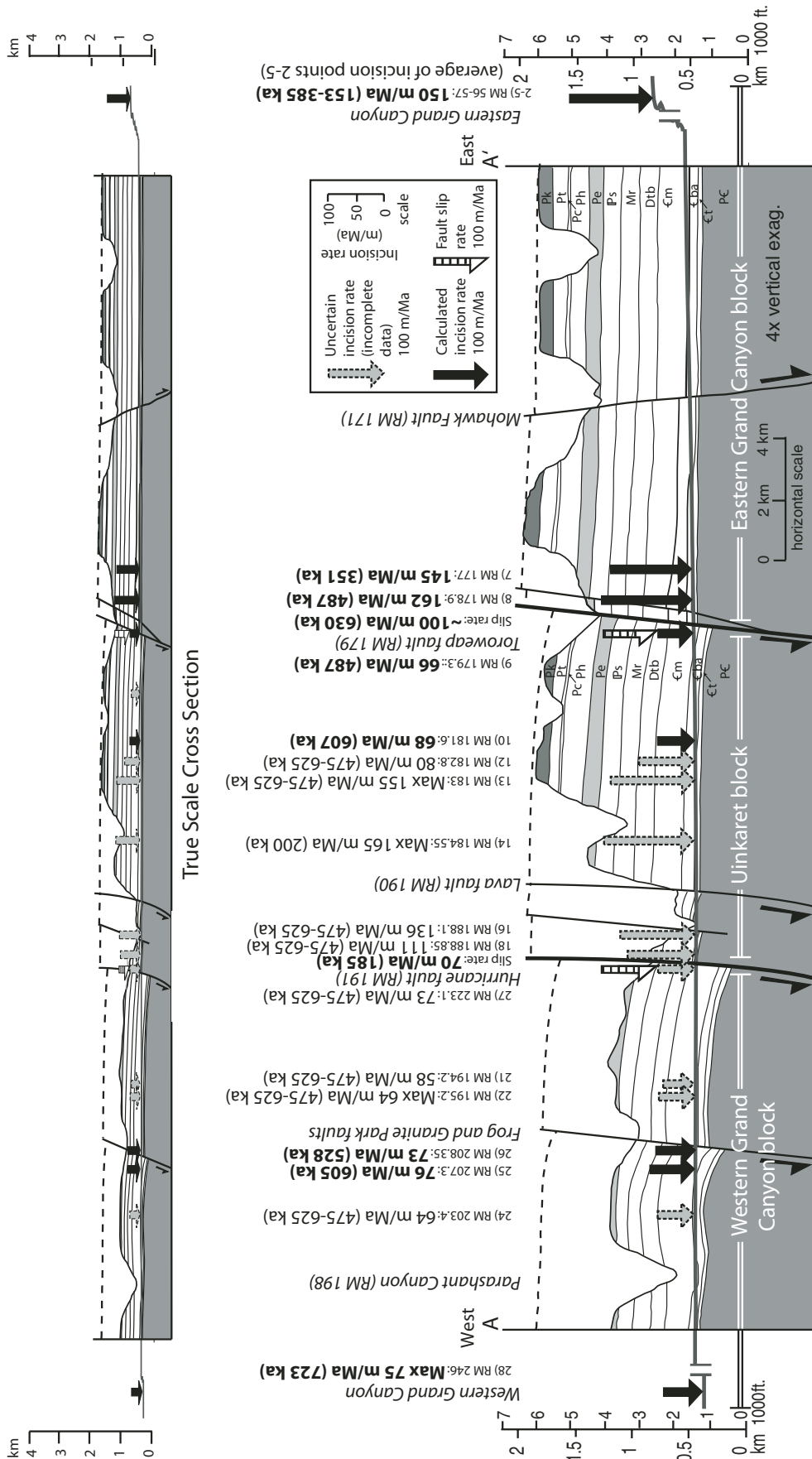
Figure 11. Incision-rate data and fault-dampened differential river incision model for Grand Canyon. Projected river gradient and canyon rim shown on E–W cross section of western Grand Canyon (location shown in Fig. 1). Eastern Grand Canyon block shows a fairly uniform incision rate of 145–162 m/Ma from RM 57 to RM 179. Uinkaret block shows diminished apparent incision (58–66 m/Ma) at east end, increasing to near the eastern canyon rate at west end, interpreted to indicate that slip on Toroweap fault is being accommodated by active formation of a hanging-wall anticline. Western Grand Canyon block also shows lowest apparent incision rates (<58 m/Ma) in immediate hanging wall of Hurricane fault, but rates increase to only 76 m/Ma, indicating that lowered rates are the result of both formation of a hanging-wall anticline and lowering of western block by 75–100 m/Ma relative to eastern Grand Canyon block. See Table 2 for description of each data point and Figure 9 for graphical portrayal of uncertainties for vectors.

TABLE 2. QUATERNARY INCISION RATES (IR) IN GRAND CANYON* AND UNCERTAINTIES

IP number	RM	Name	D	Age (ka) ±2σ	Strath height (m)	Sample height (m)	MeanPD (m)	MaxPD (m)	MaxBD (m)	IR − 2σ max m/Ma	IR p m/Ma	IR + 2σ min m/Ma	IR mean PD m/Ma	IR max BD m/Ma	Notes
1	56L	Travertine		119 ± 2	<0	26	13	23	28	197	193	190	109	235	Maximum incision rate, travertine in upper M4? deposit; Pederson et al., 2006; sparse gravels, mainly hillslope colluvium
2	56L	Travertine		153 ± 3	<0	5	13	23	28	152	150	148	85	183	Maximum incision rate, travertine drape on bedrock that extends to river level; Pederson et al., 2006; sparse pebbles in sandy deposit below travertine near river
3	57L	Travertine		385 ± 14	36	38	13	22	28	156	151	145	127	166	Pederson et al., 2006, age is mean of two analyses, new heights (2006); travertine drape covers gravels 2 m above strath
4	57L	Travertine		343 ± 28	23	24	13	22	28	143	131	121	105	149	Pederson et al., 2006; age is mean of two analyses, new heights (2006), travertine rind on m-scale river clast at strath
5	57L	Travertine		283 ± 14	24	24	13	22	28	168	163	158	131	184	Pederson et al., 2006, travertine cemented gravels inset into M5, 12 m lower strath than #3
6	57L	Travertine		125 ± 2	14	14	13	22	28	295	288	281	216	336	Maximum incision rate; Pederson et al., 2006, new heights (this paper), lowest strath in stepped sequence; mostly colluvium, minor amount of gravel above strath
7	177.3L	177 remnant*	−2	351 ± 25 n = 3	32	36	11	19	28	156	145	136	123	171	Modified from Pederson et al., 2002, pillows of basalt in river sand and gravel resting on strath
8	178.9R	Toroweap C	−0	487 ± 48 n = 1	60	~74	11	19	28	180	162	148	146	181	Toroweap fault—upthrown side, gravel above strath and below basalt is mostly non-volcanic clasts
9	179.3R	Toroweap C	1	487 ± 48 n = 1	13	~14.5	11	19	28	73	66	60	49	84	Toroweap fault—downthrown side, 1.5-m-thick gravel at distance 500 m west of fault, thicker gravel at fault (~25 m)
10	181.6R	Ponderosa	4	607 ± 48 n = 2	22	46	11	19	28	73	68	63	54	82	607 ± 48 Ponderosa remnant of Dalrymple and Hamblin (1998); flow underlain by gravel, cinders, colluvium
11	182.5R	Lava Falls	5	No date	21	28.6	12	19	28	84	73	64	60	89	Assumed age of 475–625 ka based on LIDAR heights of top and bottom of flow

(continued)

TABLE 2. QUATERNARY INCISION RATES (IR) IN GRAND CANYON* AND UNCERTAINTIES (*continued*)

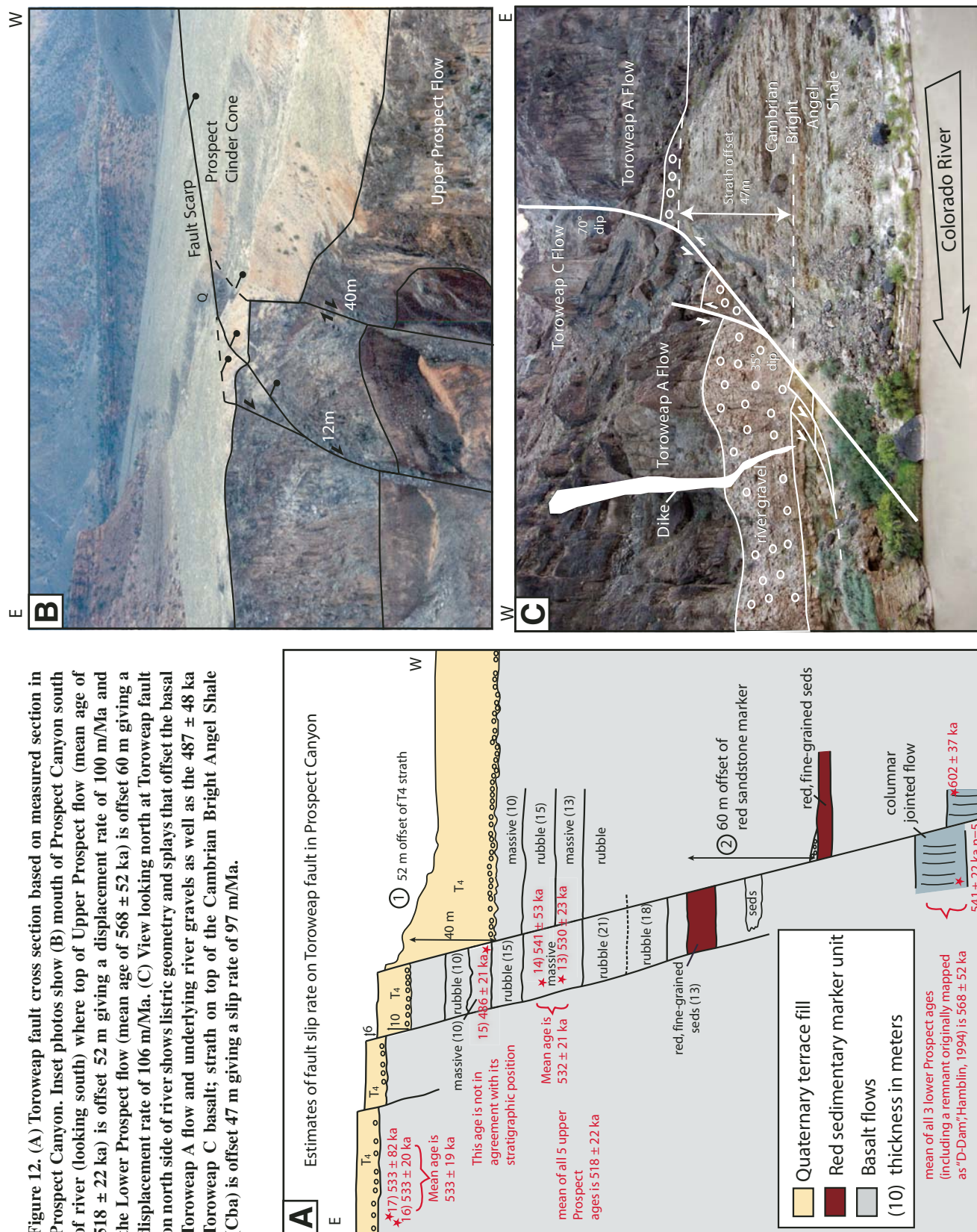| IP number	RM	Name	D	Age (ka) ±2σ	Strath height (m)	Sample height (m)	MeanPD (m)	MaxPD (m)	MaxBD (m)	IR −2σ max m/Ma	IR p m/Ma	IR +2σ min m/Ma	IR mean PD m/Ma	IR max BD m/Ma	Notes
12	182.8R	Lava Falls	5	No date	25	25	12	19	28	93	80	70	67	96	Fractured basalt mixed with river sand and silt fills a channel-like feature, flow also tops main stem river gravels, assumed age of 475–625 ka based on LIDAR heights of top and bottom of flow
13	183R	*Buried Canyon*	6	No date	66	66	12	19	28	179	155	136	142	171	*Maximum incision rate, base of flow covered by talus; assumed age of 475–625 ka based on LIDAR heights of top and bottom of flow*
14	184.55L	*Gray Ledge**	8	200 ± 72 n = 1	<15	21	12	19	28	258	165	123	130	210	*Maximum incision rate, Black Ledge remnant of Hamblin (1994), but too young, LIDAR flow top heights similar to 200 ka layered diabase on the opposite side of the river*
15	187.9L	*Gray Ledge*	12	194 ± 39 n = 1	0	0	11	18	28	116	93	77	57	144	*Lower flow (at river level) is 194 ± 39, may be slumped, base of upper flow separated from lower flow by basaltic river gravels, strath height 11 m at west end of outcrop, but strath is below river level at east end; not used in incision calculations because of uncertainty in geologic context*
16	188.1R	Black Ledge *	12	No date	56	64	11	19	28	158	136	120	122	153	3 m of main stem river gravels, 3 m of colluvium, 2.5 m of tephra under flow; assumed age of 475–625 ka based on LIDAR heights of top and bottom of flow
17	188.1R	*Gray Ledge*	12	97 ± 26 n = 1	<13	15	11	19	28	451	330	260	247	423	*Maximum incision rate, 12.5 m to first basalt rich gravel (no strath)*
18	188.85L	*Black Ledge*	12	No date	42	75-68	11	19	28	128	111	98	96	127	Field relationships complex—multiple flows and straths; massive flow correlated to 483 ± 80 ka Ar/Ar date of Fenton et al., 2004
19	189.1L	*Gray Ledge*	12	127 ± 27 n = 2	<7	10	11	19	28	260	205	169	142	276	*Maximum incision rate, 8 m to lowest gravel @ 7000 cfs (90% basalt clasts—no strath)*
20	192L	*Layered Diabase*	13	332 ± 39 n = 2	<18	18	11	19	28	126	111	100	87	139	*Maximum incision rate, basalt rests directly on bedrock*
21	194.2R	*Black Ledge*	16	No date	13	22	11	19	28	67	58	51	44	75	Assumed age of 475–625 ka based on LIDAR heights of top and bottom of flow
22	**195.2R**	***Massive Diabase***	**18**	**298 ± 57 n = 1**	**<7**	**7**	**11**	**19**	**28**	**79**	**64**	**54**	**37**	**94**	***Maximum incision rate, LIDAR height to base of flow, flow rests directly on bedrock***

(*continued*)

TABLE 2. QUATERNARY INCISION RATES (IR) IN GRAND CANYON* AND UNCERTAINTIES *(continued)*

IP number	RM	Name	D	Age (ka) ±2σ	Strath height (m)	Sample height (m)	MeanPD (m)	MaxPD (m)	MaxBD (m)	IR −2σ max m/Ma	IR p m/Ma	IR +2σ min m/Ma	IR mean PD m/Ma	IR max BD m/Ma	Notes
23	195.3L	Black Ledge	18	No date	10	11.75	11	19	28	61	53	46	38	69	Assumed age of 475–625 ka based on LIDAR heights of top and bottom of flow
24	203.4R	Black Ledge	24	No date	17	21	11	18	28	74	64	56	51	82	Assumed age of 475–625 ka based on LIDAR heights of top and bottom of flow, river gravels 10% basalt including exotic clasts
25	207.3L	**Black Ledge**	21	605 ± 12 n = 2	25	28.5	12	21	28	78	**76**	75	61	88	**Ar/Ar date from Lucchitta et al., 2000, height to strath measured in 2002, flow underlain by 3.5 m of main stem river gravels including exotic clasts**
26	208.35R	**Black Ledge**	20	528 ± 39 n = 2	20	34.5	12	20	28	82	**76**	71	61	91	**Heights to strath and base of basalt remeasured in 2006, previous measurements vary from 24–22 m**
27	223.1R	Black Ledge	12	No date	16	16	12	24	28	84	73	64	51	80	0.25 m of mainstem river gravel under flow, assumed age of 475–625 ka based on LIDAR heights of top and bottom of flow
28	**246R**	***Black Ledge***	39	*723 ± 31 n = 1*	*<30*	*<30*	*12*	*24*	*28*	*78*	*75*	*72*	*58*	*80*	***Height from Spencer Canyon Dam Survey—approximately 100' to strath from river level and depth to bedrock is 12 m***
29	290L	Sandy Point		4410 ± 30	105	107	15		28	27	27	27			Sandy Point basalt; age from Faulds et al., 2001; approximate height of basalt above river from Lucchita (1972), based on Longwell, assumed pool depth is 15 m
30	425R	Panda gravels		5500	43		65		28		20				Strath at base of Panda gravels, Panda Gulch (House et al., 2005, p. 367); >65-m depth to bedrock 7 km upstream at Davis Dam
		Average Eastern Grand Canyon Rates (**bold** rates)								159	150	143	119	172	
		Average Western Grand Canyon Rates (**bold** rates)								80	73	67	54	87	

Note: IP—incision point; RM—river mile below Lees Ferry (R—river right; L—river left); D—distance west of Toroweap fault; strath and sample height relative to 10,000 cfs level; PD—pool depth; BD—bedrock depth; IR—incision rate; IR p—preferred incision rate.
*Bold—best constrained incision rates; italics—maximum incision rates.

Figure 12. (A) Toroweap fault cross section based on measured section in Prospect Canyon. Inset photos show (B) mouth of Prospect Canyon south of river (looking south) where top of Upper Prospect flow (mean age of 518 ± 22 ka) is offset 52 m giving a displacement rate of 100 m/Ma and the Lower Prospect flow (mean age of 568 ± 52 ka) is offset 60 m giving a displacement rate of 106 m/Ma. (C) View looking north at Toroweap fault on north side of river shows listric geometry and splays that offset the basal Toroweap A flow and underlying river gravels as well as the 487 ± 48 ka Toroweap C basalt; strath on top of the Cambrian Bright Angel Shale (Cba) is offset 47 m giving a slip rate of 97 m/Ma.

B

W — E

Fault Scarp

Prospect Cinder Cone

Q

40m

12m

Upper Prospect Flow

C

W — E

Toroweap C Flow

Toroweap A Flow

Dike

Toroweap A Flow

70° dip

35° dip

river gravel

Strath offset 47m

Cambrian Bright Angel Shale

Colorado River

A

E — W

Estimates of fault slip rate on Toroweap fault in Prospect Canyon

① 52 m offset of T4 strath

40 m

T4

T4

J6

|10

T4

★(17) 533 ± 82 ka
★(16) 533 ± 20 ka
Mean age is 533 ± 19 ka

massive (10) rubble (10)
rubble (15)

15) 486 ± 21 ka
This age is not in agreement with its stratigraphic position

★ 14) 541 ± 53 ka
★ 13) 530 ± 23 ka
massive

Mean age is 532 ± 21 ka

mean of all 5 upper Prospect ages is 518 ± 22 ka

massive (10)
rubble (15)
massive (13)
rubble

rubble (21)
rubble (18)

seds

red, fine-grained seds (13)

② 60 m offset of red sandstone marker

red, fine-grained seds

columnar jointed flow

★602 ± 37 ka

541 ± 22 ka n=5
★

mean of all 3 lower Prospect ages (including a remnant originally mapped as "D-Dam", Hamblin, 1994) is 568 ± 52 ka

Quaternary terrace fill

Red sedimentary marker unit

Basalt flows

(10) thickness in meters

their stratigraphic position, with the exception of #15, the 486 ± 21 flow, as discussed above. If this sample is ignored, using the mean age of the Upper Prospect flows as 533 ka, and a displacement of 52 m, yields a displacement rate of 98 m/Ma. For Toroweap C flow on the north side of the river near Lava Falls (Fig. 12C), this flow overlies Toroweap A flow and the underlying gravels and gives a minimum age for the strath. The strath is offset 47 m, about the same amount as Toroweap C flow (Hamblin, 1994; Fig. 27), giving a slip rate (over 487 ± 48 ka) of 97 m/Ma. These rates of 97–106 m/Ma are similar to the 111 ± 9-m/Ma rates reported by Fenton et al. (2001). Thus, we interpret the displacement rate in the last 600 ka to have been ~100 m/Ma, and to have been fairly uniform through this time interval (Hamblin, 1970a; Fenton et al., 2001), rather than accelerating (Jackson, 1990).

The Toroweap fault dips 60–65° west based on its map trace as it crosses the canyon (Huntoon et al., 1981). Direct measurements in Prospect Canyon and along the river show an overall dip of ~65°, with low angle splays of ~35° (Fig. 12C). Thus, a displacement rate of 100 m/Ma slip translates to a throw (vertical component of dip slip) of ~90 m/Ma of the western block. However, our new results indicate that this Quaternary displacement is mainly taken up by formation of a hanging-wall flexure in the Uinkaret half graben, as documented by variable apparent incision rates (Fig. 11) and slight upriver dip of the 500- to 600-ka flow surfaces determined from LIDAR analysis (Crow et al., 2007). The development of eastward dips of up to 10–18° on the Paleozoic strata (Wenrich et al, 1997) may be explainable by progressive development of a hanging-wall rollover anticline over the last several million years of normal faulting with steady slip rates, but there may have also been a preexisting Laramide flexure along the Toroweap fault in this locality (Hamblin, 1994).

Hurricane Fault

The Hurricane fault has a history of Laramide west-up (reverse) motion (Naeser et al., 1989; Kelley et al., 2001; Huntoon, 2003), including reactivated reverse fault segments (Figs. 4B and 13B). It has a complicated geometry with numerous segments along its >250-km-long strike length (Stenner et al., 1999) as well as anastomosing strands within Grand Canyon region and complex variation of displacement along and across them (Huntoon et al., 1981; Wenrich et al., 1997). In general, the Hurricane fault has more offset and is older to the north and less offset and is younger to the south. In Grand Canyon, net west-down stratigraphic separation of Paleozoic units is 400–500 m in the Whitmore segment immediately north of the Colorado River,

250–400 m in the area where it crosses the Colorado River (near RM 191; Figure 4B; Wenrich et al., 1997, 1981), and 730 m in the Three Springs area ~20 km to the south (Huntoon et al., 1981).

The amount of Neogene slip has been difficult to quantify. Some workers have proposed minimal Quaternary displacement; for example, Huntoon et al. (1981) and Hamblin (1994) mapped the trace of the main Hurricane fault as covered by unfaulted remnants of the Gray Ledge (100–200 ka) and Whitmore flows (300–350 ka; Fig. 4B), suggesting that the Hurricane fault has no post–350-ka displacement. However, Billingsley (2001) reported offset of 610 m on both the 3.6 ± 0.18-ka Bundyville basalt, and for the directly underlying Mesozoic strata, yielding a displacement rate of 169 m/Ma north of Grand Canyon. The amount of Laramide reverse offset remains unconstrained, but if one assumed there were no Laramide west-up ancestry, this would suggest that most of the displacement has taken place in the last 3.6 Ma. Amoroso et al. (2004) found that slip rates of 150–250 m/Ma were relatively constant since 1 Ma in the Shivwits section of the Hurricane fault just north of the Grand Canyon. Recent seismicity attests to continued activity.

Fenton et al. (2001) estimated an average displacement rate of 81 ± 6 m/Ma over approximately the last 200 ka, based on He cosmogenic surface dates and offsets of Whitmore Cascade (177 ± 9-ka) and Bar Ten (88 ± 6-ka) flows and young alluvial fans (29–74 ka). We measured fault displacement of 14 m (Fig. 4B) of a thick, columnar-jointed flow in Whitmore Canyon (Fig. 13A); $^{40}Ar/^{39}Ar$ dating of fallen basalt columns that are probably from this flow give 186 ± 26 ka (Table 1; Raucci, 2004), providing a displacement rate of 75 m/Ma in the last 186 ka. We have also identified new splays of the Hurricane fault system with Quaternary displacement along and east of the river near RM 190 (Fig. 4B). The fault west of the river displaces Whitmore-age remnants by 6 m; the fault east of the river has west-down offset of an alluvial deposit (Qfd4 of Fenton et al., 2004) that overlies the 319-ka Whitmore flow, with displacement varying from 10 to 15 m along the fault. These new displacements (Fig. 4B), if added to the 14 m along the strand in Whitmore Wash (Fig. 13B), give a cumulative slip of 30–35 m in the last 200–320 ka, and a minimum slip rate of 94–109 m/Ma. Further studies of the partitioning of displacement between strands will be needed to refine these estimates, but we use the range 75–100 m/Ma as our current best estimate of late Quaternary slip rate on the Hurricane fault.

Figure 14 summarizes the combined incision- and slip-rate data. For the Hurricane fault, like the

Toroweap fault, Paleozoic rocks define a hanging-wall anticline that formed at least in part due to Quaternary slip on listric faults. But, unlike the Toroweap block, this is not as strongly indicated by apparent incision-rate data. Additional dating is needed to decipher the extent of hanging-wall flexure in this area. Apparent incision rates west of the Hurricane fault do not return to rates of eastern Grand Canyon and instead are fairly constant at 60–75 m/Ma (Fig. 14). Based on differential incision rates, this suggests that the western Grand Canyon block has subsided vertically ~100 m/Ma relative to the eastern Grand Canyon block, mainly due to movement along the Hurricane fault system, which may have been active longer (3–4 Ma) than the Toroweap fault (2–3 Ma) as Neogene extension has migrated eastward into the Colorado Plateau (Jackson, 1990).

Western Faults

There are also a number of small faults between the Hurricane and Grand Wash faults (Table DR2). For example, Resor (2007) identified 275 m of normal slip and accompanying flexure across the Frogy fault system (RM 196.4). Huntoon et al. (1981, 1982) mapped approximately 45 faults that cross the river between RM 225 and 275. A majority of these faults have west-up displacement (550 m net separation) that probably took place during Laramide contraction; some have west-down displacement (185 m net west-down separation) and are likely Miocene. The net displacement from these faults is ~365 m of west-up separation. The amount of Quaternary slip on these faults is unconstrained, but any contribution these faults make to lowered apparent incision rates in western Grand Canyon is less than the resolution of our existing data (Fig. 14).

The physiographic boundary between the Colorado Plateau and Basin and Range provinces is the Grand Wash cliffs, which marks the abrupt western end of Grand Canyon (Fig. 1). This is a retreating escarpment of Paleozoic rocks formed initially by movement on the Grand Wash fault zone pre-10 Ma (Beard, 1996; Brady et al., 2000; Faulds et al., 2001). Grand Wash fault zone separates the flat-lying strata of the Colorado Plateau from the east-dipping 30–50° Paleozoic strata of the Wheeler Ridge block (Brady et al., 2000). There is ~3.5 km of stratigraphic separation across this zone, and strata of the Wheeler Ridge block are folded into a hanging-wall flexure expressed in both the Paleozoic rocks and Neogene rocks. The traces of the Grand Wash fault strands are covered by unfaulted Muddy Creek Formation, indicating that movement ceased before ca. 10 Ma (Beard, 1996; Brady et al., 2000; Faulds et al., 2001).
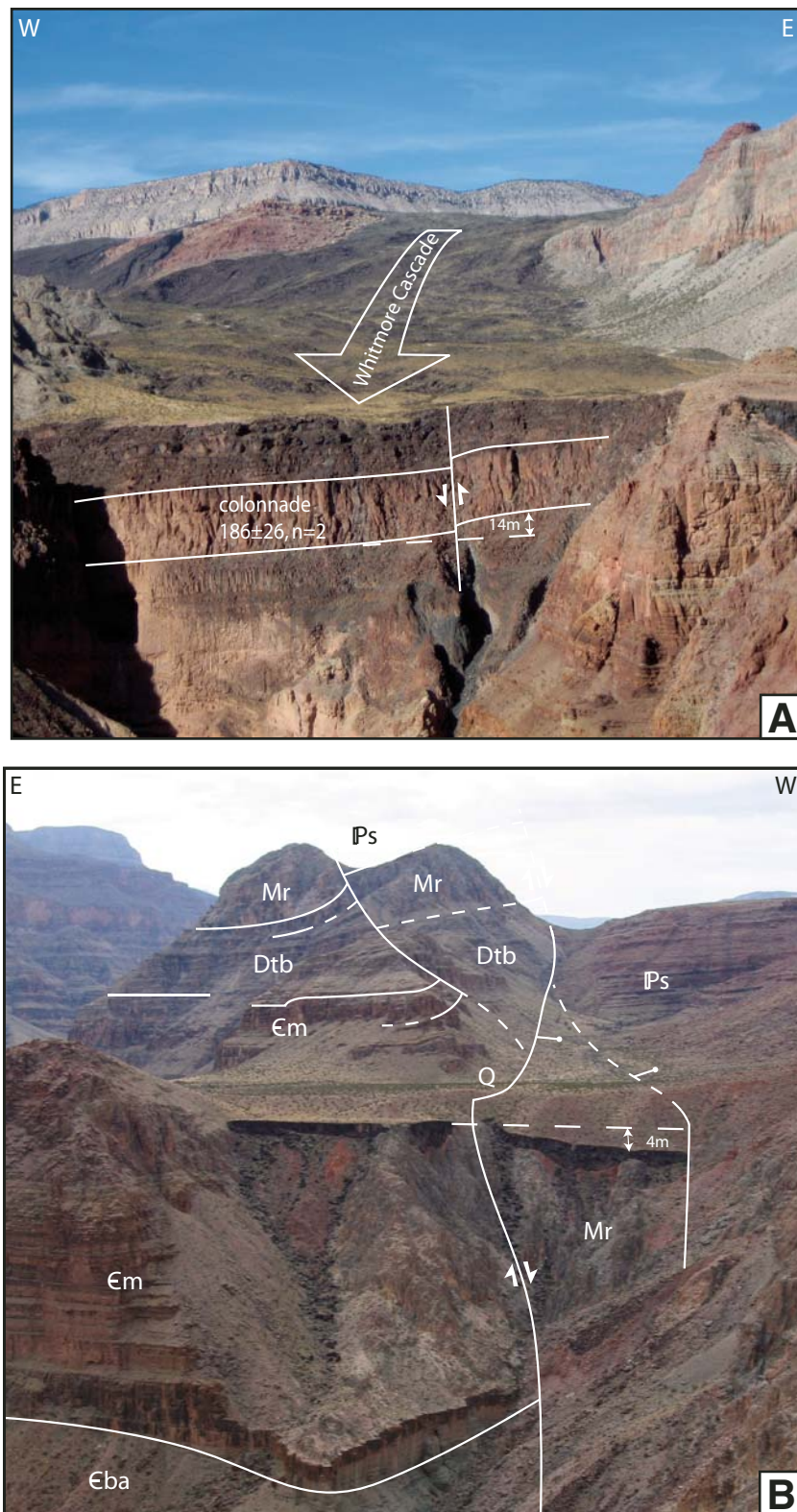
Figure 13. Photos of offset basalts along Hurricane fault in Whitmore Canyon. (A) Looking north, 186 ± 26 colonnade flow is offset ~14 m (including flexure) giving slip rate of 75 m/Ma. (B) Looking south, offset of ~4 m of Quaternary surface (51 ± 9; Fenton et al., 2001) and highest Whitmore flow gives displacement rate of 80 m/Ma; syncline in footwall of one strand of Hurricane fault suggests Laramide contractional ancestry to this strand (shown as reverse fault in Fig. 4B) before extensional reactivation to produce the observed normal separation.

The Wheeler fault is a 60°-west-dipping normal fault (Longwell, 1936) that is exposed ~5 km west of the Grand Wash fault zone. It has ~2.5 km of normal stratigraphic separation of Paleozoic rocks (Brady et al., 2000). The Wheeler fault splits into several faults to the south, and these show ~300 m (Brady et al., 2000) to 450 m (Howard and Bohannon, 2001) of normal separation on the top of the Hualapai limestone. Paleozoic rocks, the Hualapai limestone, and the 4.7-Ma Grand Wash basalts above the Wheeler fault all have east-dips defining a hanging-wall flexure (Howard and Bohannon, 2001). Paleozoic rocks dip 30–40° whereas Hualapai limestone dips <5°. Both slip amount and hanging-wall dip suggest that most slip took place before 6 Ma (Howard and Bohannon, 2001), although there is also significant Neogene slip that is important for regional models (below).

The Iceberg Canyon fault, an additional 5 km west (mapped before the filling of Lake Mead; Longwell, 1936), is a 10°–35°–west-dipping, listric, normal fault. It has ~1.2 km of normal separation (Brady et al., 2000). Based on the lower elevation of the 4.4-Ma Sandy Point basalt (105 m above pre-dam river grade) relative to the 4.7-Ma Grand Wash basalts (Howard and Bohannon, 2001), the base of which is up to 260 m above pre-dam river grade, we infer that some post–4.4-Ma slip took place on faults between the Wheeler and Iceberg Canyon fault systems. However, pending further mapping, we lump all post–6-Ma displacements to be part of the combined Wheeler/Iceberg Canyon fault systems.

Refined Model for Differential Incision of Grand Canyon Due to Fault Dampening

The new data on incision- and fault-slip rates confirms and significantly refines the model presented by Pederson and Karlstrom (2001) and Pederson et al. (2002b) that west-down displacement on Neogene normal faults in the western Grand Canyon dampens the eastern Grand Canyon incision rate. The original model (Pederson and Karlstrom, 2001; Pederson et al., 2002b) was:

footwall incision rate = (apparent hanging-wall incision rate) + (fault-slip rate). (1)

This works well in the immediate vicinity of the Toroweap fault, where the incision rate in the footwall (two closest rates upstream of the fault in Fig. 9) averages 154 m/Ma over the last 500 ka and is subequal to the sum of the average incision rate in the immediate hanging wall of 67 m/Ma (two closest), plus the fault-slip rate of ~100 m/Ma. Across the Hurricane fault,
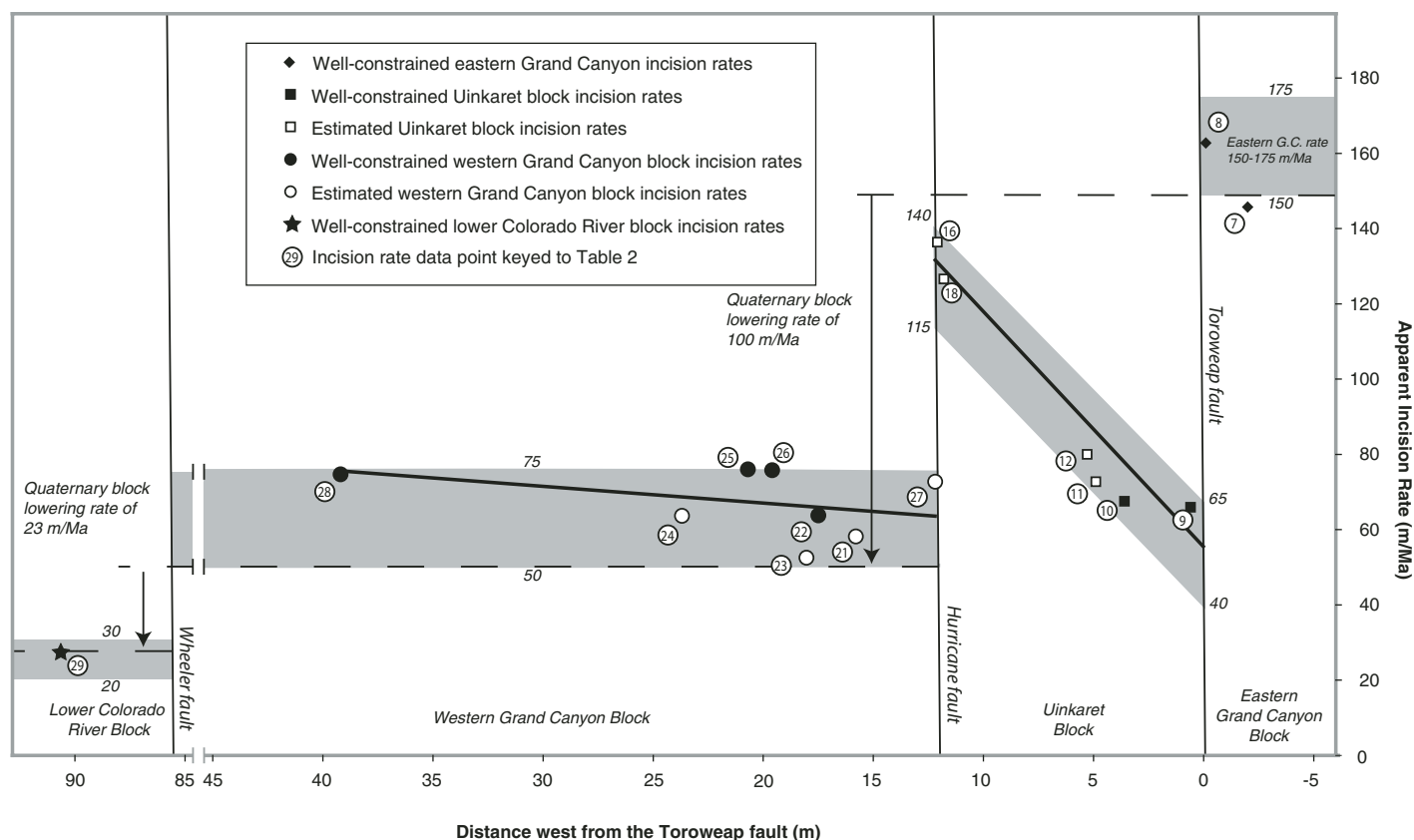
Figure 14. Plot of incision rate versus distance west of the Toroweap fault. Variation in apparent incision rates indicates variable subsidence west of the Toroweap fault due to formation of a hanging-wall anticline above a listric fault.

the relationship also works well: the footwall rate of 131 m/Ma (average of two closest) over approximately the last 550 ka is subequal to the downstream incision rate of 61 m/Ma (two closest) plus fault-slip rate of 75–100 m/Ma.

A refinement of the model addresses what parts of fault slip are accommodated by hanging-wall flexure versus relative vertical-block subsidence, and helps explain the effects of multiple faults dampening a far-field incision rate, and with faults operating over different time spans (Fig. 15A). By our original hypothesis, the combined slip on the faults of 175–200 m/Ma would suggest that apparent incision rates west of both faults would be zero or negative, resulting in the river that should be aggrading. This is not supported by observations for positive bedrock incision of 50–75 m/Ma at all known locations and over all time scales as western blocks have been moving down relative to eastern blocks. This apparent discrepancy can be explained by a revised model:

footwall-incision rate = (apparent hanging-wall incision rate) + [(vertical-block lowering rate) + (slip rate accommodated by hanging-wall flexure)].   (2)
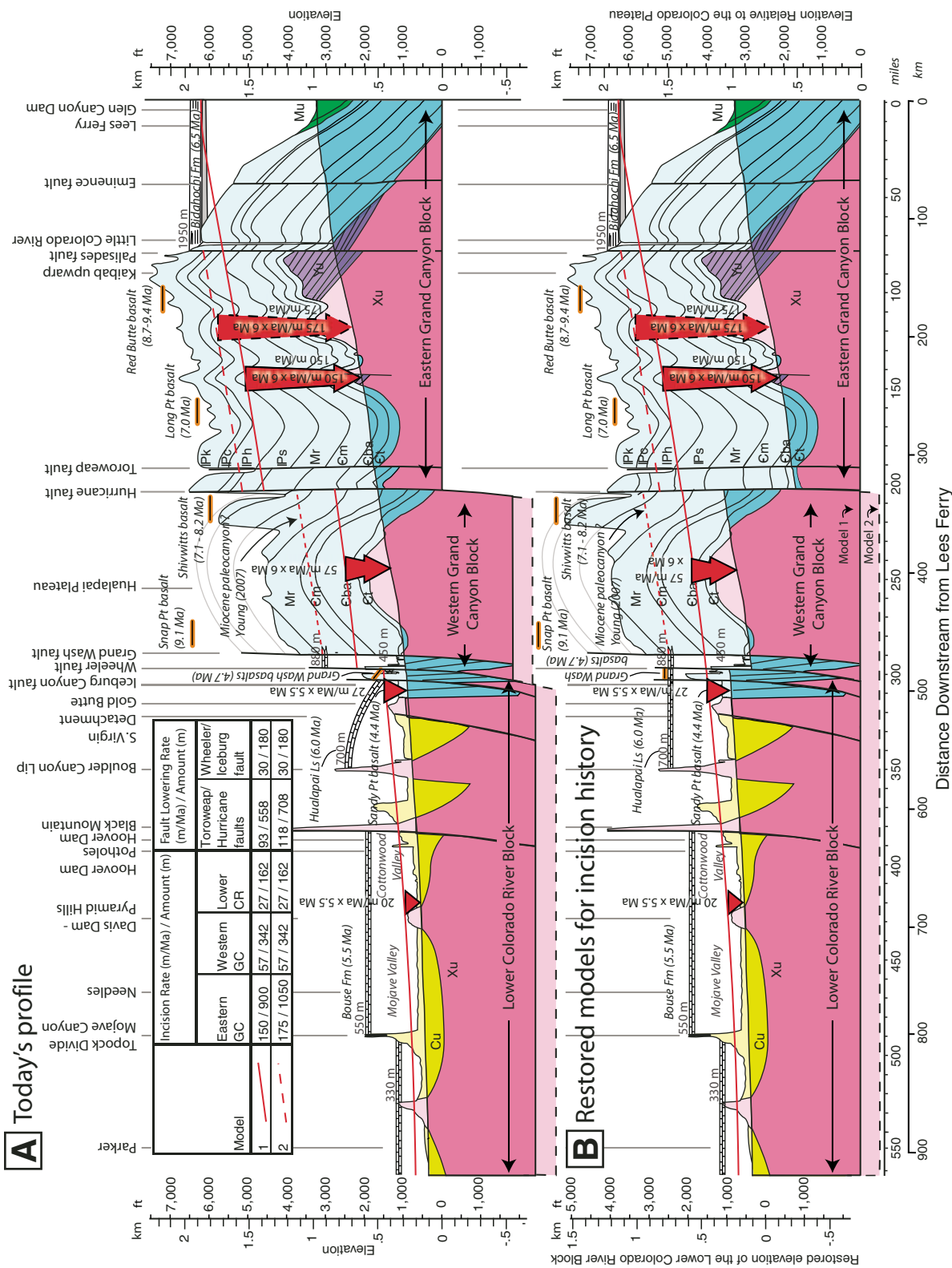
As shown in Figure 14, hanging-wall flexure in the Uinkaret block accounts for much of the incision dampening, with overall block lowering of only ~10–20 m/Ma for the estimated slip of 100 m/Ma. West of the Hurricane fault, the importance of hanging-wall flexure is less (~10 m/Ma), with vertical block lowering of 60–90 m/Ma accounting for most of the postulated slip rate (75–100 m/Ma). For the Wheeler fault, of the ~400 m of offset of the 6-Ma Hualapai Limestone (Howard and Bohannon, 2001), about half is taken up by hanging-wall flexure (Fig. 15A). These data suggest that different amounts of the total fault slip are partitioned into hanging-wall flexure due to differing geometries and histories of the fault systems.

Long-Term Incision Models for Grand Canyon

Over longer time spans, fault displacement data and apparent incision rates from the Basin and Range province suggest that the fault dampening model and coherent block behavior of fault blocks has operated for the last 6 Ma. Given the pre-dam strath height of 105 m (Lucchitta, 1972), average rate of incision at Sandy Point

(RM 295) over the last 4.41 ± 0.03 Ma (Faulds et al., 2001) is 27 m/Ma (Fig. 15; Table 2). Although less well constrained, bedrock incision rate in the last 6 Ma in the Mojave Valley of the Lower Colorado River is ~20 m/Ma (Fig. 15). As reported by House et al. (2005), the first Colorado River gravels, the Panda gravels, fill paleovalleys cut into Miocene pre-Colorado River alluvial fan deposits at ~43 m above the present river in an area just a few km south of Davis Dam. Depth to bedrock at the dam is >65 m based on data from dam construction (Bahmoier, 1950). These data suggest apparent incision rates for the Lower Colorado River block of ~20 m/Ma, shown in Figure 15A, and suggest that this Basin and Range block has moved down ~180 m (~30 m/Ma) relative to the western Grand Canyon block since 6 Ma.

The data from the Lower Colorado River block (4.4–5.5 Ma) cover a different time frame than our new data from the Grand Canyon (approximately the last 720 ka). It is unlikely that incision was constant from 6 Ma to present due to expected changes in climatic, geomorphic, and tectonic conditions, but there are few data that link the incision histories between the early history and our late Quaternary data. One

Figure 15. (A) Colorado River longitudinal profile with projected bedrock units in Grand Canyon; pink—Precambrian basement, blue—Paleozoic strata, green—Mesozoic strata, yellow—Cenozoic deposits; schematic representation of geologic units modified from Moores (in LaRue, 1925); note ~10 times vertical exaggeration. Today's river profile shown with three blocks defined by internally consistent apparent incision rates—eastern Grand Canyon, western Grand Canyon, Lower Colorado River block. Red lines represent amount of incision in 6 Ma modeled by extending Quaternary rates back in time. (B) Fault-dampened incision model restores fault slips and models hypothetical river paleoprofile at 6 Ma using equation for Model 2 (see text). Models 1 and 2 differ in terms of amount of fault lowering on the combined Hurricane/Toroweap faults system needed to match 150–175 m/Ma incision rates in eastern Grand Canyon. For these models, the Lower Colorado River block has been lowered 738–888 m (respectively) on normal faults since 6 Ma relative to eastern Grand Canyon block.

approach, supported by our data, that bedrock incision rates in Grand Canyon have been steady over approximately the last 720 ka, is to extrapolate Quaternary incision rates back in time to provide at least a first-order comparison of incision histories at short and long time scales.

Figure 15A is drawn with scaled incision vectors drawn at six times the vertical scale of the river profile such that vectors show the amount of bedrock incision that would have occurred over the last 6 Ma at Quaternary rates, compared to the depth of Grand Canyon. The upper (dashed) line in Figure 15A shows 6 Ma of bedrock incision in eastern Grand Canyon at 175 m/Ma (from the regressed line of Fig. 10); the lower (solid) line shows 6 Ma of bedrock incision at 150 m/Ma (using maximum pool depth from Fig. 9). Thus, Quaternary incision rates, extrapolated back 6 Ma, can explain approximately two-thirds of the present depth of eastern Grand Canyon (Fig. 15A). For western Grand Canyon block, fault-dampened Quaternary incision rates, extrapolated back 6 Ma (solid line), would explain only approximately one-third of the depth of western Grand Canyon.

This 200- to 400-m "incision discrepancy" in eastern Grand Canyon and 700- to 900-m discrepancy in western Grand Canyon might be used to argue that our reported Quaternary rates are underestimates. Hanks et al. (2001; Hanks and Blair, 2003) reported Quaternary rates of ~500 m/Ma in Glen Canyon in the last 500 ka, and Marchetti and Cerling (2001) reported rates of 380–480 m/Ma in approximately the last 200 ka in the Fremont River tributary of the Colorado River. But, if incision has taken place at these rates in Grand Canyon, this would require present bedrock depths to be an additional 80 m deeper (to get to 300 m/Ma over 500 ka) than our mean pool depth, which is not supported by any existing drilling measurements of maximum depth to bedrock (Fig. 8). One possibility is that the published Glen Canyon and Fremont River rates are overestimates because the cosmogenic surface ages used are minimum ages, perhaps beyond the useful 100- to 200-ka window for surface ages (Wolkowinsky and Granger, 2004). This interpretation is supported by the rates of 140 m/Ma reported on the San Juan River based on cosmogenic burial dating (Wolkowinsky and Granger, 2004). Hence, the difference between the needed long-term average eastern Grand Canyon incision rate of 275 m/Ma and our data for Quaternary rates of 150–175 m/Ma seems *unlikely* to be explained in terms of an underestimate of late Quaternary rates (c.f. Hanks et al., 2001).

Instead, the "incision discrepancy" is best explained by a combination of non-steady, decelerating incision rates and the existence of previously carved canyons that were used during integration of the Colorado River. Exploring the first option, steady rates of 275 m/Ma would be needed to carve eastern Grand Canyon (up to 1650 m deep) in 6 Ma. Pre-Grand Canyon, 7- to 10-Ma basalts near the rim of Grand Canyon also provide an approximate incision/denudation datum. South of Grand Canyon, the 8.8- to 9.7- Ma Red Butte basalt rests on Chinle Formation (without river gravels) at an elevation of 2160 m, and the 7.0-Ma Long Point basalt overlies Eocene gravels at an elevation of ~1900 m. North of Grand Canyon, the 7.1- to 8.2- Ma Shivwitts basalts rest on Kaibab and Moenkopi formations at elevations of ~1800 m and the 9.1-Ma Snap Point basalt rests on Kaibab Formation at an elevation of 1950 m (Billingsley, 2001) . Assuming the basalts flowed into relative low spots in the landscape at 7–9 Ma, this basalt datum also suggests a long-term incision/denudation rate of ~250 m/Ma over this time interval (Fig. 15A). To explain the difference between the inferred long-term rates and the observed Quaternary rates, we envision that rapid base level fall for Colorado Plateau drainages took place over a geologically short time interval after initial integration of the system ca. 6 Ma. This led to early incision rates >250-300 m/Ma, with a subsequent decline in incision rates as channel slopes decreased, leading to Quaternary incision values of 150–175 m/Ma.

Another contributing factor to explain the incision discrepancy, especially in western Grand Canyon (Fig. 15A), is that initial integration of the Colorado River from the Colorado Plateau to the Basin and Range may have taken advantage of previously carved canyons. Young (2001, 2007 and references therein) has documented paleocanyons (Peach Springs, Milkweed-Hindu), up to 1000 m deep, that existed in the Eocene to middle Miocene and contained north-flowing rivers that drained the Mogollon highlands. These canyons were part of an extensive Paleogene drainage system possibly involving the ancestral Salt River (Potochnik, 2001) and other deep Miocene canyons that were reused during drainage reversal and integration of the present drainage system. Similarly, several workers have postulated that western Grand Canyon, in general, and the Esplanade surface, in particular, may have been partly carved before 6 Ma (Scarborough, 2001), perhaps by early drainages that flowed west from the Kaibab uplift (Young, 2001, 2007). In particular, Young (2007) proposed a Miocene canyon >600 m deep that was present in western Grand Canyon, having developed in part due to structural relief from normal faulting on the Grand Wash fault system 16.5–10 Ma (Fig. 15A). The top of the 6-Ma Hualapai limestone, at an elevation of 880 m, is inferred to be near its original depositional elevation relative to the Colorado Plateau block (Howard and Bohannon, 2001) and may have been the lake level fed by Miocene drainages (Young, 2007). The elevation of the base of the well-documented canyons near Peach Springs is 1100–1200 m (Young, 2001). Together these data (dotted line in Fig. 15A) suggest that perhaps half of the 700- to 900-m "incision discrepancy" in western Grand Canyon may be explained by the existence of such paleocanyons (Fig. 15B), although the history of which paleocanyons were used and how they were linked remains unconstrained.

Restored Paleoprofiles

Figure 15B restores the profile in Figure 15A by removing fault slip according to model parameters in the table (upper left of Fig. 15) to arrive at a modeled 6-Ma river profile. These models keep three parameters fixed: (1) the range of eastern Grand Canyon incision rates is fixed at 150–175 m/Ma to conform to Figures 9 and 10; (2) fault lowering on the Wheeler/Iceberg Canyon fault is fixed at 180 m over the last 6 Ma (30 m/Ma) based on observations of offset and flexure of the Hualapai Limestone (Howard and Bohannon, 2001); (3) fault lowering on the combined Toroweap and Hurricane faults are considered together for simplicity (and to conform to Fig. 14). Two possible fault-dampened incision models are shown. In the two models, apparent incision rates of 57 and 27 m/Ma for the western Grand Canyon and Lower Colorado River blocks, respectively, can restore to match the 150- and 175-m/Ma eastern Grand Canyon incision rates via 93 and 118 m/Ma of fault lowering active over 6 Ma on the combined Hurricane/Toroweap fault system. These models demonstrate that the fault-dampened incision model is capable of explaining observed data to first order, especially if the "incision discrepancy" throughout Grand Canyon can be explained by higher 5- to 6-Ma incision rates in combination with the existence of western paleocanyons. These models suggest a cumulative vertical displacement of 750–900 m between the Lower Colorado block and the eastern Grand Canyon block in the last 6 Ma; this displacement is needed to explain the Quaternary incision rate data.

More refined models will require better data on temporal and spatial partitioning of slip among different fault strands, as well as refined apparent incision rates and their variation through time. In Models 1 and 2 (Fig. 15), slip on the combined Toroweap and Hurricane faults was modeled to last for the total 6 Ma of canyon incision. Shorter durations for fault slip, as perhaps suggested by geologic data (if one

assumes no Laramide reverse slip, see above), require larger fault displacements on multiple strands of the Hurricane than shown in Figure 15. Because of the downstream cumulative effects of fault slip, models that restrict slip to the Toroweap to 2 Ma and slip on the Hurricane to 3.5 Ma, to accomplish the observed incision dampening, also require larger slip on the Wheeler/Iceberg Canyon fault systems. In spite of remaining uncertainties regarding the temporal and spatial variations of both fault slip and apparent incision rates, the differential incision model provides a powerful new constraint that needs to be addressed when framing the controversy about the long-term evolution of the Colorado River system and uplift models for the Colorado Plateau.

Evaluating Models for River Integration

Figure 16A extends the modeled 5- to 6-Ma paleoriver profile to sea level at the Gulf of California, which has formed the base level for the river since 5.36 Ma. The premise of this analysis is that the river profile of major rivers like the Colorado, although they evolve through time, may be used as an approximate datum for estimating uplift and denudation rates. At largest scale, and million-year time frame, rivers evolve toward a concave-up profile that reflects a balance between channel slope, discharge, and sediment load (e.g., Bull, 1979, 1991). Even in young, large rivers in tectonically active landscapes (Burbank et al., 1996), this basic form establishes itself early, albeit with knickpoints and steep gradients that reflect disequilibrium. Large rivers have ample stream power to erode and essentially erase small fault scarps and spill-over points in short time spans (Pederson et al., 2003).

Figure 16A shows a river profile that may have resulted from initial integration by progressive lake spill over (stepped red line), a model that is supported by emerging geochronology. This profile depicts spill over from Lake Bidahochi at ca. 6.5 Ma (Scarborough 2001; Meek and Douglas, 2001), integration of drainage through a Miocene paleocanyon that may have existed west of the Kaibab uplift (Young, 2007), arrival of water to Lake Hualapai at ca. 6 Ma (House et al., 2005; Spencer and Pearthree, 2001), arrival of water at Lake Mojave at 5.5 Ma (House et al., 2005), followed closely by overtopping of Topock gorge to fill Lake Havasu and Lake Blythe at ca. 5.5 Ma (House et al., 2005; Spencer et al., 2007), with Colorado Plateau sediments reaching the Gulf of California at 5.36 Ma (Dorsey et al., 2005). As discussed above, this hypothetical 5- to 6-Ma paleoprofile is 200–300 m higher than the modeled

paleoprofile reconstructed using steady Quaternary incision and slip rates, a difference that may be explainable by higher 5- to 6-Ma incision rates that would likely have resulted from rapid adjustment of the stream profile to the new knickpoints (spill-over points). The integration process probably involved both spill over (Scarborough 2001; Spencer and Pearthree, 2001) and headward erosion (Lucchitta, 1990). Headward erosion, aided by groundwater sapping and resulting stream piracy (Pederson, 2001), was likely also an important mechanism to connect and integrate paleocanyons during initial integration of the Colorado River system across the Grand Wash cliffs and Kaibab uplift.

Evaluating Alternative Uplift Models

The post–6-Ma evolution of the Colorado River profile can be considered in terms of two end-member uplift models (Fig. 16B). In both, we assume that by 5–6 Ma the river was developing a regionally concave-up profile from the east side of the Kaibab uplift to the Gulf of California. The models coincide upstream of the Davis Dam-Mojave Valley area, our last firm incision point (Fig. 16A). Upstream of this point, the fault-dampening model seems to explain the differential incision data over the last 6 Ma, albeit needing the resolutions for the "incision discrepancy" discussed above. The two models differ in how the 5- to 6-Ma Colorado River profile may have been graded to sea level in late Miocene time south of the Mojave basin. The Lower Colorado River region is structurally complex near Yuma because of the San Andreas fault system (including the Algodones fault, Fig. 16A), but most workers have noted an absence of Quaternary normal faulting in much of the Lower Colorado River corridor (House et al., 2005). Although early Colorado River gravels (units A and B of Metzger et al., 1973) are present both at the surface and in the subsurface between Mojave Valley and Yuma, we know of no definitive strath at the base of the first Colorado River gravels such as exists in the Mojave Valley region. The following discussion highlights the importance of continued neotectonic and geomorphic studies of the Lower Colorado River region to help evaluate whether faulting across the Plateau-Basin and Range boundary caused the Colorado Plateau to go up (Fig. 16B, Model 1), or the 5- to 6-Ma, sea-level datum to go down (Fig. 16B, Model 2) relative to today's mean sea level.

As shown in Figure 16B, Model 1 lets the river profile evolve by keeping the left side (sea level) relatively fixed and allowing uplift of the Colorado Plateau (e.g., Powell, 1875; Dutton, 1882; Lucchitta, 1972, 1979; Sahagian et

al., 2002). It assumes that much of the Lower Colorado River profile has remained close to sea level (Metzger, 1968; Lucchitta et al., 2001), with minor vertical movements on faults related to the San Andreas system. Note that global sea level was 10–20 m higher during the early Pliocene warm period (5–3 Ma; Ravelo et al., 2004), such that global changes in sea level are not a major consideration for this time period.

Model 1 is supported by the observations that bedrock straths are observed *above* the present river level in many places. The presence of Colorado River gravels (by themselves) at elevations up to 250 m above the present river (House et al., 2005) is likely due to the history of aggradation from 5.5 to 3.3 Ma followed by a series of aggradation and incision events (Metzger et al., 1973, House et al., 2005). However, the observation that bedrock straths for these various events are commonly above the modern river level and at progressively lower elevations between Lake Mead and Yuma may suggest modest but still positive bedrock incision for the entire length of the profile (House et al., 2005), as shown in Model 1. For example, early Colorado River gravels near Blythe (Unit B, correlated by House et al. (2005) with the >4-Ma gravels of Bullhead City) rest on bedrock at elevations up to 150 m above current river level. Model 1 suggests a stepped, but regionally concave-up, profile for the newly integrated 5- to 6-Ma Colorado River and is compatible with a relative lack of late Miocene to Quaternary faulting and subsidence between Davis Dam and Parker (House et al., 2005). As a driver for Model 1, epeirogenic uplift of the Colorado Plateau is consistent with geodynamic models that suggest that a component of extension and plateau uplift in the southwestern USA is taking place via ongoing mantle-driven surface uplift (Karlstrom et al., 2005).

Model 2 keeps the right side of Figure 16B fixed, consistent with models for no Neogene surface uplift of the Colorado Plateau (Spencer, 1996; Spencer and Patchett, 1997; Pederson et al., 2002a), and lowers the western end of the 6-Ma river profile and the 5- to 6-Ma, sea-level datum relative to the fixed Colorado Plateau elevation. This model requires that the paleo–6-Ma sea-level position is now ~800 m below present sea level near Yuma and that post–6-Ma history of the lower Colorado River corridor was strongly aggradational. In this model, Bouse Formation that was encountered at 150 m depths in drill holes (Howard and Bohannon, 2001) near Yuma would have to be non-marine saline lake deposits, well above paleo-sea level (Spencer and Patchett, 1997; Patchett and Spencer, 2001). The Bouse/Imperial Formations south of Yuma interfinger with Colorado River gravels
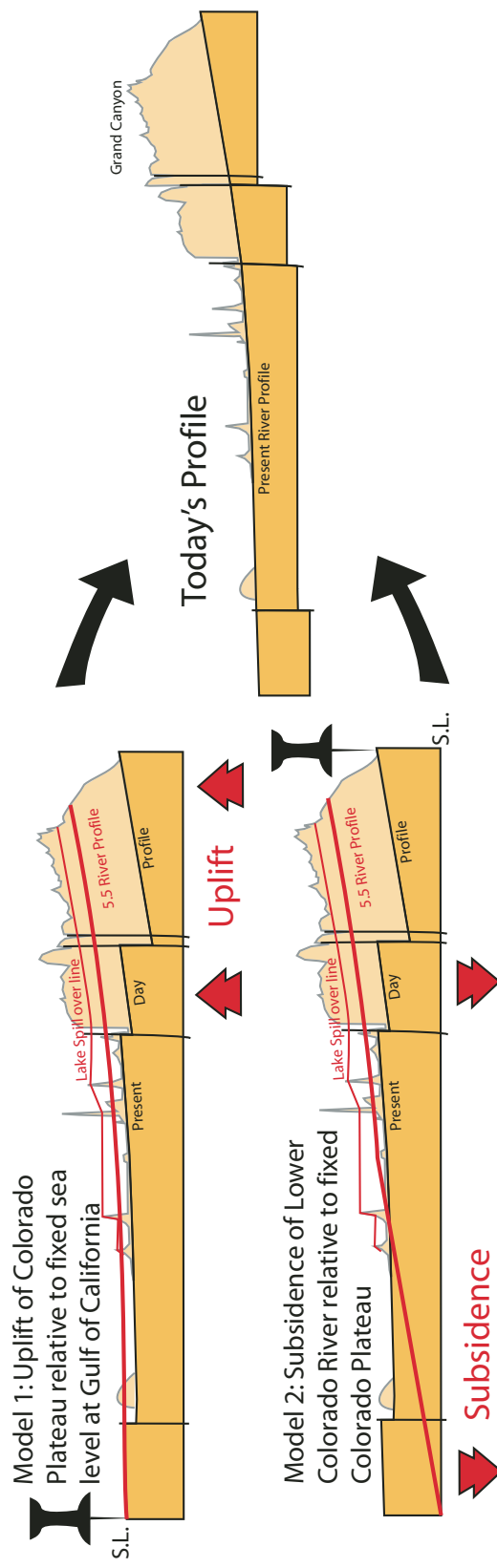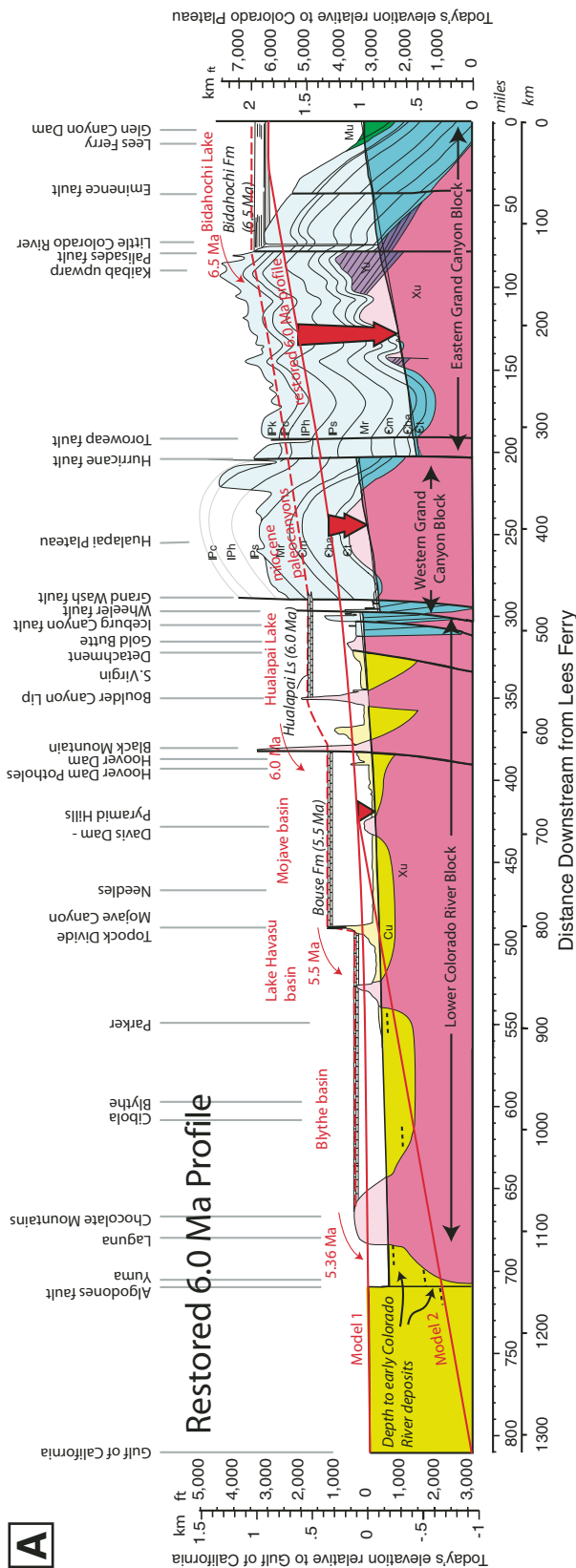
Figure 16. Summary of regional fault displacement model and long-term evolution for the Colorado River. Progressive lake spill over (stepped red line) from Bidahochi Lake (6.5 Ma), to Hualapai Lake (6 Ma) to Mojave and Blythe basins (5.5 Ma) may have facilitated drainage integration across the Kaibab uplift and Grand Wash cliffs and establishment of the Colorado River profile along its present course by 5.36 Ma. (A) Restoration of Neogene fault displacement using Model 1 of Figure 15, and assuming steady Quaternary incision rates, results in a reasonable 6-Ma paleoprofile (as in Fig. 15), but with a several hundred meter discrepancy with the inferred 5.5-Ma lake spill-over profile (see text). Dashed lines at the left are depths to possible early Colorado River deposits as interpreted by Olmstead et al. (1973) and Metzger et al. (1973). (B) Below Mojave basin, alternate uplift/subsidence models imply—Model 1: ~750–900 m uplift of Colorado Plateau relative to sea level, versus Model 2: ~750–900 m of subsidence of the late Miocene sea-level datum at the Gulf of California.

(Buising, 1990) and sit on marine rocks at up to 1000 m below sea level (Olmstead et al., 1973), but these are on the other side of the San Andreas fault, the vertical motion across which remains poorly constrained. Model 2 may be supported by possible early Colorado River gravels (units A and B of Metzger) and the pre-Colorado River Bouse Formation encountered at various depths in drill holes (Olmstead et al., 1973; Metzger et al., 1973; Spencer et al., 2007), as shown in Figure 16A, although we know of no definitive 5- to 6-Ma Colorado River straths that have been positively identified.

Model 2 would require a change, somewhere south of Mojave Valley, from a river profile to the north that has had modest net incision since 6 Ma (20–30 m/Ma), to a 5- to 6-Ma river profile datum to the south that has subsided markedly below sea level in the last 6 Ma. The reported variable depths of the pre-Colorado units suggest vertical components of fault displacement on the Algodones of several hundred meters (Olmstead et al., 1973), but even restoring this offset (Fig. 16) does not create a reasonable concave-up, 5- to 6-Ma, paleoriver profile for Model 2. Thus, if Model 2 is correct, there would have to be other, presently unrecognized, Neogene faults along the profile that would allow reconstruction of a reasonable 5- to 6-Ma profile, the gradient for which, in this downstream part of the profile, must have been lower than upstream gradients.

Aspects of each model remain viable, and components of each may have operated. For example, there may have been several hundred meters of actual uplift of eastern blocks accompanied by similar magnitude subsidence in the Gulf region. Nevertheless, the combined geologic data (profile analysis, bedrock straths above the modern river level, and reported absence of Quaternary faulting in most of the Lower Colorado River corridor) seem best explained by Model 1, where most of the 750–900 m of relative displacement resulted from surface uplift of the Colorado Plateau.

CONCLUSIONS

New ^{40}Ar/^{39}Ar dates on basalts in western Grand Canyon provide one of the best records of canyon incision in the world. Different apparent incision rates in different reaches of Grand Canyon, when combined with new fault-slip rates, lead to our new model for fault-dampened incision and provide first-order constraints on how active faulting interacts with the incision of a major river/canyon system. Dated basalt flows and travertine deposits associated with old river gravels indicate average incision rates of 150–175 m/Ma for the 290-km-long eastern

Grand Canyon block (Lees Ferry to Toroweap fault) over the last 350 ka. The Uinkaret block (8-km-wide block from Toroweap to Hurricane faults) shows variable bedrock incision rates: 66 m/Ma in the immediate hanging wall of the Toroweap fault increasing westward to 136 m/Ma in the immediate footwall of the Hurricane fault. This suggests that fault-dampened incision in this block is being accomplished mainly by formation of a hanging-wall anticline above a listric Toroweap fault. The western Grand Canyon block (140-km-wide block from Hurricane to Grand Wash faults) shows bedrock incision rates of 50–75 m/Ma over the last 723 ka. This is less than half of the eastern canyon rate and indicates lowering of western Grand Canyon block by ~100 m/Ma relative to the eastern Grand Canyon block over the last 723 ka. New dates on offset basalts indicate ~100 m/Ma slip rate on the Toroweap fault (last 600 ka) and 70- to 100-m/Ma slip on the Hurricane fault (last 186 ka). This requires modification of previous models for fault-dampened incision. In our new model, slip rate plus downstream incision rate are subequal to upstream rates only immediately across faults. At longer spatial scales, approximately half of the cumulative slip on these two faults (170–200 m/Ma) is expressed as relative vertical displacement between the Colorado Plateau and Basin and Range blocks, the rest being accommodated by flexure of the hanging walls. Mechanistically, this is due to a listric character of Neogene normal faulting combined with partitioning of slip between fault strands.

Dated basalts and new data on neotectonic fault block geometry provide insight on longer term incision history of Grand Canyon and processes at the boundary between the Colorado Plateau and Basin and Range provinces. Throughout Grand Canyon, Quaternary bedrock incision rates appear to have been nearly constant in a given reach for the last 720 ka, but these are minimum rates for long-term canyon incision, which requires ~275 m/Ma to carve eastern Grand Canyon in 6 Ma. Long-term average apparent incision rates in the upper Lake Mead region of ~27 m/Ma in the last 4.4 Ma and ~20 m/Ma in the last 5.5 Ma near Davis Dam also suggest coherent block behavior of the Colorado River corridor block and net incision for the entire profile north of the Mojave Valley. Using steady incision rates and preliminary models, the Colorado River corridor block has lowered ~27 m/Ma relative to the western Grand Canyon block, which, in turn, has been lowering at ~100 m/Ma relative to the Colorado Plateau averaged over 6 Ma. The combined fault displacement caused 750–900 m of relative vertical displacement between the Basin and Range and Colorado Plateau provinces in the last 6 Ma.

Of the two models, surface uplift of the Colorado Plateau by 750–900 m better reconstructs a reasonable 6-Ma paleoprofile and better explains straths that are above sea level between the Mojave Valley and Yuma. Such Quaternary epeirogenic uplift may have been driven by buoyant low-velocity mantle upwelling beneath the tectonically active western United States.

REFERENCES CITED

Amoroso, L., Pearthree, P.A., and Arrowsmith, J.R., 2004, Paleoseismicity and neotectonics of the Shivwits section of the Hurricane Fault, northwestern Arizona: Bulletin of the Seismological Society of America, v. 94, no. 5, p. 1919–1942, doi: 10.1785/012003241.

Anders, M.D., Pederson, J.L., Rittenour, T.M., Sharp, W.D., Gosse, J.C., Karlstrom, K.E., Crossey, L.J., Goble, R.J., Stockli, L.J., and Yang, G., 2005, Pleistocene geomorphology and geochronology of eastern Grand Canyon: Linkages of landscape components during climate changes: Quaternary Science Reviews, v. 24, p. 2428–2448, doi: 10.1016/j.quascirev.2005.03.015.

Bahmoier, H.F., 1950, Construction engineering problems at Davis Dam: Los Angeles, California, Advance copy of paper presented at the 1950 Spring Meeting of the American Society of Civil Engineers, April 26–29.

Beard, L.S., 1996, Paleogeography of the Horse Spring Formation in relation to the Lake Mead fault system, Virgin Mountains, Nevada and Arizona, *in* Beratan, K.K., ed., Reconstructing the history of Basin and Range extension using sedimentology and stratigraphy: Boulder, Colorado, Geological Society of America Special Paper 303, p. 27–60.

Best, M.G., McKee, E.H., and Damon, P.E., 1980, Space-time-composition patterns of late Cenozoic mafic volcanism, southwestern Utah and adjoining areas: American Journal of Science, v. 280, p. 1035–1050.

Beus, S.S., and Morales, M., 2003, Grand Canyon geology, second edition: New York, Oxford University Press, 432 p.

Billingsley, G.H., 2001, Volcanic rocks of the Grand Canyon area, *in* Young, R.A., and Spamer, E.E., eds., Colorado River: Origin and evolution: Grand Canyon, Arizona, Grand Canyon Association, p. 223–229.

Brady, R., Wernicke, B., and Fryxell, J., 2000, Kinematic evolution of a large-offset continental normal fault system, South Virgin Mountains, Nevada: Geological Society of America Bulletin, v. 112, no. 9, p. 1375–1397, doi: 10.1130/0016-7606(2000)112<1375:KEOALO> 2.0.CO;2.

Brumbaugh, D.S., 1987, A tectonic boundary for the southern Colorado Plateau: Tectonophysics, v. 136, p. 125–136, doi: 10.1016/0040-1951(87)90335-0.

Buising, A.V., 1990, The Bouse Formation and bracketing units, southeastern California and western Arizona: Implications for the evolution of the proto-Gulf of California and the lower Colorado River: Journal of Geophysical Research, v. 95, p. 20,111–20,132.

Bull, W.B., 1979, Threshold of critical power in streams: Geological Society of America Bulletin, v. 90, p. 453–464, doi: 10.1130/0016-7606(1979)90<453:TOCPIS>2.0.CO;2.

Bull, W.B., 1991, Geomorphic responses to climate change: New York, Oxford University Press, 326 p.

Burbank, D.W., Leland, J., Fielding, E., Anderson, R.S., Brozovic, N., Ried, M.R., and Duncan, C., 1996, Bedrock incision, rock uplift, and threshold hillslopes in the northwestern Himalayas: Nature, v. 379, p. 505–510, doi: 10.1038/379505a0.

Crow, R.S., Karlstrom, K. E., McIntosh, W., Dunbar, N., Peters, L., and Pederson, J., 2007, History of Quaternary volcanism and lava dams in western Grand Canyon based on LIDAR analysis, ^{40}Ar/^{39}Ar dating, and field studies: Implications for flow stratigraphy, timing of volcanic events, lava dam structure, and interaction of volcanism and canyon incision: in press.

Dalrymple, G.B., and Hamblin, W.K., 1998, K-Ar ages of Pleistocene lava dams in the Grand Canyon in Arizona: Proceedings of the National Academy of Sciences of the United States of America, v. 95, no. 17, p. 9744–9749, doi: 10.1073/pnas.95.17.9744.

Dorsey, R.J., Fluette, A., McDougall, K., Housen, B.A., and Janecke, S.U., 2005, Terminal Miocene arrival of Colorado River sand in the Salton Trough, southern California: Implications for initiation of the lower Colorado River drainage: Geological Society of America Annual Meeting and Exposition, Abstracts with Programs, p. 109.

Dutton, C.E., 1882, The Tertiary history of the Grand Canyon district: U.S. Geological Survey Monograph 2, 264 p.

Faulds, J.E., Price, L.M., and Wallace, M.A., 2001, Pre-Colorado paleogeography and extension along the Colorado Plateau-Basin and Range boundary, northwest Arizona, *in* Young, R.A., and Spamer, E.E., eds., Colorado River: Origin and evolution: Grand Canyon, Arizona,-Grand Canyon Association, p. 93–99.

Fenton, C.R., Webb, R.H., Pearthree, P.A., Cerling, T.E., and Poreda, R.J., 2001, Displacement rates on the Toroweap and Hurricane faults: Implications for Quaternary downcutting in the Grand Canyon, Arizona: Geology, v. 29, no. 11, p. 1035–1038, doi: 10.1130/0091-7613(2001)029<1035:DROTTA>2.0.CO;2.

Fenton, C.R., Poreda, R.J., Nash, B.P., Webb, R.H., and Cerling, T.E., 2004, Geochemical discrimination of five Pleistocene lava-dam outburst-flood deposits, western Grand Canyon, Arizona: The Journal of Geology, v. 112, p. 91–110, doi: 10.1086/379694.

Hamblin, W.K., 1970a, Structure of the western Grand Canyon region, *in* Hamblin, W.K., and Best, M.G., eds., The western Grand Canyon District: Utah Geological Society Guidebook to the Geology of Utah, no. 23, p. 3–19.

Hamblin, W.K., 1970b, Late Cenozoic basalts of the western Grand Canyon, *in* Hamblin, W.K., and Best, M.G., eds., The western Grand Canyon District: Utah Geological Society Guidebook to the Geology of Utah, no. 23, p. 21–37.

Hamblin, W.K., 1974, Late Cenozoic volcanism in the western Grand Canyon, *in* Breed, W.J., and Roat, E.C., eds., Geology of the Grand Canyon: Museum of Northern Arizona/Grand Canyon National History Association, p. 142-170.

Hamblin, W.K., 1994, Late Cenozoic lava dams in the western Grand Canyon: Geological Society of America Memoir 183, 139 p.

Hamblin, W.K., Damon, P.E., and Bull, W.B., 1981, Estimates of vertical crustal strain rates along the western margins of the Colorado Plateau: Geology, v. 9, no. 7, p. 293–298, doi: 10.1130/0091-7613(1981)9<293:EOVCSR>2.0.CO;2.

Hanks, T.C., and Blair, L.J., 2003, Differential incision of the Grand Canyon related to Quaternary faulting—Constraints from U-series and Ar-Ar dating: Comment: Geology, June 2003, v. 31, p. e16-17.

Hanks, T.C., and Webb, R.H., 2006, Effects of tributary debris on the longitudinal profile of the Colorado River in Grand Canyon: Journal of Geophysical Research, v. 111, F02020, 13 p., doi:10.1029/2004JF000257,2006,

Hanks, T.C., Lucchitta, I., Davis, S.W., Davis, M.E., Finkel, R.C., Lefton, S.A., and Garvin, C.D., 2001, The Colorado River and the age of Glen Canyon, *in* Young, R.A., and Spamer, E.E., eds., Colorado River: Origin and evolution: Grand Canyon, Arizona, Grand Canyon Association, p. 29–134.

House, P.K., Pearthree, P.A., Howard, K.A., Bell, J.W., Perkins, M.E., Faulds, J.E., and Brock, A.L., 2005, Birth of the lower Colorado River—Stratigraphic and geomorphic evidence for the inception near the conjunction of Nevada, Arizona, and California, *in* Pederson, J.L., and Dehler, C.M., eds., Interior western United States, Field Guide 6: Boulder, Colorado, Geological Society of America, p. 357–387.

Howard, K.A., and Bohannon, R.G., 2001, Lower Colorado River: Upper Cenozoic deposits, incision, and evolution, *in* Young, R.A., and Spamer, E.E., eds., Colorado River: Origin and evolution: Grand Canyon, Arizona, Grand Canyon Association, p. 101–105.

Huntoon, P.W., 1977, Holocene faulting in the western Grand Canyon, Arizona: Geological Society of America Bulletin, v. 88, p. 1619–1622, doi: 10.1130/0016-7606(1977)88<1619:HFITWG>2.0.CO;2.

Huntoon, P.W., 2003, Post-Precambrian tectonism in the Grand Canyon region, *in* Beus, S.S., and Morales, M., eds., Grand Canyon Geology: New York, Oxford University Press, p.222–259.

Huntoon, P.W., Billingsley, G.H., and Clark, M.D., 1981, Geologic map of the Hurricane fault zone and vicinity, western Grand Canyon, Arizona: Grand Canyon Natural History Association: Grand Canyon Arizona, v. 1, p. 48,000.

Huntoon, P.W., Billingsley, G.H., and Clark, M.D., 1982, Geologic map of the Lower granite Gorge and vicinity, western Grand Canyon, Arizona: Grand Canyon Natural History Association: Grand Canyon, Arizona, scale 1:48,000.

Jackson, G., 1990, Tectonic geomorphology of the Toroweap fault, western Grand Canyon, Arizona: Implications for transgression of faulting on the Colorado Plateau: Arizona Geological Survey Open-File Report 90-4, 67 p.

Karlstrom, K.E., Whitmeyer, S.J., Dueker, K., Williams, M.L., Levander, A., Humphreys, G., Keller, G.R., and the CD-ROM Working Group, 2005, Synthesis of results from the CD-ROM experiment: 4-D image of the lithosphere beneath the Rocky Mountains and implications for understanding the evolution of continental lithosphere, *in* Karlstrom, K.E. and Keller, G.R., eds., The Rocky Mountain region–An evolving lithosphere: Tectonics, Geochemistry, and Geophysics: American Geophysical Union Geophysical Monograph, 154, p. 421–441.

Kelley, S.A., Chapin, C.E., and Karlstrom, K.E., 2001, Laramide cooling histories of the Grand Canyon, Arizona, and the Front Range, Colorado, determined from apatite fission-track thermochronology, *in* Young, R.A., and Spamer, E.E., eds., Colorado River: Origin and evolution: Grand Canyon, Arizona, Grand Canyon Association, p. 37–42.

LaRue, E.C., 1925, Water power and flood control of Colorado River below Green River: U.S. Geological Survey Water Supply Paper 556, 176 p.

Longwell, C.R., 1936, Geology of the Boulder Reservoir floor, Arizona-Nevada: Geological Society of America Bulletin, v. 47, p. 1393–1476.

Longwell, C.R., 1963, Reconnaissance geology between Lake Mead and Davis Dam, Arizona-Nevada: U.S. Geological Survey Professional Paper 374-E, 51 p.

Lucchitta, I., 1972, Early history of the Colorado River in the Basin and Range Province: Geological Society of America Bulletin, v. 83, p. 1933–1947, doi: 10.1130/0016-7606(1972)83[1933:EHOTCR]2.0.CO;2.

Lucchitta, I., 1979, Late Cenozoic uplift of the southwestern Colorado River region: Tectonophysics, v. 61, p. 63–95.

Lucchitta, I., 1990, History of the Grand Canyon and of the Colorado River in Arizona, *in* Bues, S.S., and Morales, M., eds., Grand Canyon geology: New York, Oxford University Press, p. 311–332.

Lucchitta, I., Curtis, G.H., Davis, M.E., Davis, S.W., and Turrin, B., 2000, Cyclic aggradation and downcutting, fluvial response to volcanic activity, and calibration of soil-carbonate stages in the western Grand Canyon, Arizona: Quaternary Research, v. 53, no. 1, p. 23–33, doi: 10.1006/qres.1999.2098.

Lucchitta, I., Curtis, G.H., Davis, M.E., Davis, S.W., and Turrin, B., 2001, Rates of downcutting of the Colorado River in the Grand Canyon region, *in* Young, R.A., and Spamer, E.E., eds., Colorado River: Origin and evolution: Grand Canyon, Arizona, Grand Canyon Association, p. 155–157.

McKee, E.D., and Schenk, E.T., 1942, The lower canyon lavas and related feathers at Toroweap in Grand Canyon: Journal of Geomorphology, v. 5, p. 245–273.

Marchetti, D., and Cerling, T.E., 2001, Bedrock incision rates for the Fremont River, tributary of the Colorado River, *in* Young, R.A., and Spamer, E.E., eds., Colorado River: Origin and evolution: Grand Canyon, Arizona, Grand Canyon Association, p. 125–127.

McDougall, K., Poore, R.Z., and Matti, J.C., 1999, Age and environment of the Imperial Formation near San Gorgonio Pass, California: Journal of Foraminiferal Research, v. 29, p. 4–25.

Meek, N., and Douglas, J., 2001, Lake overflow: An alternative hypothesis for Grand Canyon incision and development of the Colorado River, *in* Young, R.A., and Spamer, E.E., eds., Colorado River: Origin and evolution: Grand Canyon, Arizona, Grand Canyon Association, p. 199–206.

Merritts, D.J., Vincent, K.R., and Wohl, E.E., 1994, Long river profiles, tectonism, and eustasy: A guide to interpreting fluvial terraces: Journal of Geophysical Research, B, v. 99, p. 14,031–14,050.

Metzger, D.G., 1968, The Bouse Formation (Pliocente) of the Parker-Blytne-Cibola area, Arizona and California,: U.S.Geological Survey Professional Paper 600D, p. D126–D136.

Metzger, D.G., Loeltz, O.J., and Irelon, B., 1973, Geohydrology of the Parker-Blytne-Cibola area, Arizona and California: U.S. Geological Survey Professional Paper 486G, 130 p.

Naeser, C.W., Duddy, I.R., Elston, D.P., Dumitru, T.A., Green, P.F., and Hanshaw, P.M., 1989, Fission-track dating: Ages for Cambrian strata, and Laramide and post-middle Eocene cooling events from the Grand Canyon, Arizona, *in* Elston, D.P., Billingsley, G.H., and Young, R.A., eds., Geology of Grand Canyon, northern Arizona (with Colorado River guides): Washington, D.C., 28th International Geological Congress, American Geophysical Union, Field Trip Guidebook T115/315, p. 139-144.

Olmstead, F.H., Loeltz, O.J., and Irelan, B., 1973, Geohydrology of the Yuma area, Arizona and California: U.S. Geological Survey Professional Paper 486-H, 154 p.

Oskin, M.E., and Stock, J.M., 2003, Marine incursion synchronous with plate-boundary localization in the Gulf of California: Geology, v. 31, p. 23–26, doi: 10.1130/0091-7613(2003)031<0023:MISWPB>2.0.CO;2.

Patchett, P.J., and Spencer, J.E., 2001, Applications of Ar isotopes to the hydrology of the Colorado River system waters and potentially related Neogene sedimentary formations, *in* Young, R.A., and Spamer, E.E., eds., Colorado River: Origin and evolution: Grand Canyon, Arizona, Grand Canyon Association, p. 167–171.

Pazzaglia, F.J., and Brandon, M.T., 2001, A fluvial record of long-term steady-state uplift and erosion across the Cascadia forearc high, western Washington State: American Journal of Science, v. 301, p. 385–431.

Pazzaglia, F.J., Gardner, T.W., and Merritts, D.J., 1998, Bedrock fluvial incision and longitudinal profile development over geologic timescales determined from fluvial terraces, *in* Tinkler, K.J., and Wohl, E.E., eds., Rivers over rock: Fluvial processes in bedrock channels: American Geophysical Union Geophysical Monograph Series, v. 107, p. 207–335

Pearthree, P.A., 1998, Quaternary fault data and map for Arizona: Arizona Geological Survey Open-File Report 98-24, 122 p.

Pearthree, P.A., Menges, C.M., and Mayer, L., 1983, Distribution, recurrence, and possible tectonic implications

of late Quaternary faulting in Arizona: Arizona Bureau of Geology and Mineral Technology Open-File Report 83-20, 51 p.

Pederson, D.T., 2001, Stream piracy revisited: A groundwater sapping solution: GSA Today, v. 11, no. 9, p. 4–10, doi: 10.1130/1052-5173(2001)011<0004:SPRAGS>2.0.CO;2.

Pederson, J., and Karlstrom, K., 2001, Relating differential incision of Grand Canyon to slip along the Hurricane-Toroweap fault system, *in* Young, R.A., and Spamer, E.E., eds., Colorado River: Origin and evolution: Grand Canyon, Arizona, Grand Canyon Association, p. 159–163.

Pederson, J.L., Mackley, R.D., and Eddleman, J.L., 2002a, Colorado Plateau uplift and erosion evaluated using GIS: GSA Today, v. 12, no. 8, p. 4, doi: 10.1130/1052-5173(2002)012<0004:CPUAEE>2.0.CO;2.

Pederson, J., Karlstrom, K., McIntosh, W.C., and Sharp, W., 2002b, Differential incision of Grand Canyon related to Quaternary faulting—Data from U-series and Ar-Ar dating: Geology, v. 30, p. 739–742, doi: 10.1130/0091-7613(2002)030<0739:DIOTGC>2.0.CO;2.

Pederson, J., Karlstrom, K.E., Sharp, W., and McIntosh, W., 2003, Differential incision of the Grand Canyon related to Quaternary faulting—Constraints from U-series and Ar/Ar dating: Comment and reply: Geology, online forum, www.gsajournals.org, p. e16-e17.

Pederson, J.L., Anders, M.D., Rittenhour, T.M., Sharp, W.D., Gosse, J.C., and Karlstrom, K.E., 2006, Using fill terraces to understand incision rates and evolution of the Colorado River in eastern Grand Canyon, Arizona: Journal of Geophysical Research, v. 111, F02003, 10 p., doi 10.1029/2004JF000201.

Potochnik, A.R., 2001, Paleogeomorphic evolution of the Salt River Region: Implications for Cretaceous-Laramide inheritance for ancestral Colorado River drainage, *in* Young, R.A., and Spamer, E.E., eds., Colorado River: Origin and evolution: Grand Canyon, Arizona, Grand Canyon Association, p. 17–22.

Powell, J.W., 1875, Exploration of the Colorado River of the West and its tributaries: Washington D.C., U.S. Government Printing Office, 291 p.

Raucci, J., 2004, Structure and neotectonics of the Hurricane fault zone, western Grand Canyon, Arizona [M.S. thesis]: Flagstaff, Arizona, Northern Arizona University, 180 p.

Ravelo, A.C., Andreasen, D.H., Lyle, M., Lyle, A.O., and Wara, L.W., 2004, Regional climate shifts caused by gradual global cooling in the Pliocene epoch: Nature, v. 429, p. 263–267, doi: 10.1038/nature02567.

Renne, P.R., Swisher, C.C., Deino, A.L., Karner, D.B., Owens, T.L., and Depaolo, D.J., 1998, Intercalibration of standards: Absolute ages and uncertainties in $^{40}Ar/^{39}Ar$ dating: Chemical Geology, v. 145, p. 117–152, doi: 10.1016/S0009-2541(97)00159-9.

Resor, P.G., 2007, Deformation associated with a continental normal fault system, western Grand Canyon, Arizona: Geological Society of America Bulletin.

Sahagian, D., Proussevitch, A., and Carlson, W., 2002, Timing of Colorado Plateau uplift: Initial constraints from vesicular basalt-derived paleoelevations: Geology, v. 30, p. 807–810, doi: 10.1130/0091-7613(2002)030<0807:TOCPUI>2.0.CO;2.

Scarborough, R., 2001, Neogene development of the little Colorado River Valley and eastern Grand Canyon: Field evidence for an overtopping hypothesis, *in* Young, R.A., and Spamer, E.E., eds., Colorado River: Origin and evolution: Grand Canyon, Arizona, Grand Canyon Association, p. 207–212.

Spencer, J.E., 1996, Uplift of the Colorado Plateau due to lithosphere attenuation during Laramide low-angle subduction: Journal of Geophysical Research, v. 101, p. 13,595–13,609, doi: 10.1029/96JB00818.

Spencer, J.E., and Patchett, P.J., 1997, Sr isotope evidence for a lacustrine origin for the upper Miocene to Pliocene Bouse Formation, lower Colorado River trough, and implications for timing of Colorado Plateau uplift: Geological Society of America Bulletin, v. 109, p. 767–778, doi: 10.1130/0016-7606(1997)109<0767:SIEFAL>2.3.CO;2.

Spencer, J.E., and Pearthree, P.A., 2001, Headward erosion versus closed basin spill over as alternative causes of Neogene capture of the Ancestral Colorado River by the Gulf of California, *in* Young, R.A., and Spamer, E.E., eds., Colorado River: Origin and evolution: Grand Canyon, Arizona, Grand Canyon Association, p. 215–222.

Spencer, J.E., Pearthree, P.A., and House, P.K., 2008, Some constraints on the evolution of the latest Miocene to earliest Pliocene Bouse lake system and initiation of the lower Colorado River, *in* Reheis, M.C., Hershler, R., and Miller, D.M., eds., Late Cenozoic drainage history of the southwestern Great Basin and Lower Colorado River region: Geologic and Biotic Perspectives: Geological Society of America Special Paper 439, doi: 10.1130/2008.2439(17).

Spencer, J.E., Peters, L., McIntosh, W.C., and Patchett, P.J., 2001, $^{40}Ar/^{39}Ar$ geochronology of the Hualapai Limestone and Bouse Formation and implications for the age of the lower Colorado River, *in* Young, R.A., and Spamer, E.E., eds., Colorado River: Origin and evolution: Grand Canyon, Arizona, Grand Canyon Association, p. 89–91.

Stenner, H.D., Lund, W.R., Pearthree, P.A., and Everitt, B.L., 1999, Paleoseismologic investigations of the Hurricane fault in northwestern Arizona and southwestern Utah: Arizona Geological Survey Open-File Report 99-8, 136 p.

Stevens, L., 1983, The Colorado River in Grand Canyon: Flagstaff, Arizona, Red Lake Books, 110 p.

U.S. Geological Survey and Arizona Geological Survey, 2006, Quaternary fault and fold database for the United States, accessed February 7, 2006, from U.S. Geological Survey Web site: http//earthquake.usgs.gov/regional/qfaults/.

Wenrich, K., Billingsley, G., and Huntoon, P., 1997, Breccia pipe and geologic map of the northeastern Hualapai Indian Reservation and vicinity, Arizona: U.S. Geological Survey Geologic Investigation Series Map I-2440, scale 1:48,000.

Willis, G.C., and Biek, R.F., 2001, Quaternary incision rates of the Colorado River and major tributaries in the Colorado Plateau, Utah, *in* Young, R.A., and Spamer, E.E., eds., Colorado River: Origin and evolution: Grand Canyon, Arizona, Grand Canyon Association, p. 125–127.

Wilson, R.P., 1986, Sonar patterns of Colorado River bed, Grand Canyon, *in* Glysson, G.D., ed., Proceedings of the Fourth Federal Interagency Sedimentation Conference (two volumes): Tucson, Arizona, Interagency Advisory Commission on Water Data, Subcommittee on Sedimentation, p. 5.133–5.142.

Wolkowinsky, A.J., and Granger, D.E., 2004, Early Pleistocene incision of the San Juan River, Utah, dated with ^{26}Al and ^{10}Be: Geology, v. 32, p. 749–752, doi: 10.1130/G20541.1.

Young, R.A., 2001, The Laramide-Paleogene history of the western Grand Canyon region: Setting the stage, *in* Young, R.A., and Spamer, E.E., eds., Colorado River: Origin and evolution: Grand Canyon, Arizona, Grand Canyon Association, p. 7–15.

Young, R.A., 2008, Pre–Colorado River drainage in western Grand Canyon: Potential influence on Miocene stratigraphy in Grand Wash trough, *in* Reheis, M.C., Hershler, R., and Miller, D.M., eds., Late Cenozoic Drainage History of the Southwestern Great Basin and Lower Colorado River Region: Geologic and Biotic Perspectives: Geological Society of America Special Paper 439, doi: 10.1130/2008.2439(14).

Young, R.A., and Spamer, E.E., 2001, Colorado River: Origin and evolution: Grand Canyon, Arizona, Grand Canyon Association, 280 p.

Statement of Ownership, Management, and Circulation
(Required by Title 39 U.S.C. 4369)

The Geological Society of America Bulletin (Publication No. 0016-7606) is published bi-monthly by The Geological Society of America, Inc., (GSA) with headquarters and offices at 3300 Penrose Place, Boulder, Colorado 80301 U.S.A.; and mailing address of Post Office Box 9140, Boulder, Colorado 80301-9140 U.S.A. The Publisher is Jon Olsen; offices and mailing addresses are the same as above. The annual subscription prices are: GSA Members $82; GSA Associate-Student Members $42; non-members $650. The publication is wholly owned by The Geological Society of America, Inc., a not-for-profit, charitable corporation. No known stockholder holds 1 percent or more of the total stock. CEDE & Company, 55 Water Street, New York, NY 10041, holds all outstanding bonds; there are no known mortgagees or holders of other securities. The purpose, function, and nonprofit status of The Geological Society of America, Inc., has not changed during the preceding twelve months. The average number of copies of each issue during the preceding twelve months and the actual number of copies published nearest to the filing date (September 2006 issue) are noted at right.

This information taken from PS Form 3526, signed 14 September 2007 by the Publisher, Jon Olsen, and filed with the United States Postal Service in Boulder, Colorado.

Item No. from PS Form 3526	Extent and Nature of Circulation	Avg. No. Copies Each Issue in past 12 Months	Actual No. Copies of Single Issue Published Nearest to Filing Date
a.	Total No. Copies (Net press run)	3,700	3,800
b.	Paid and/or Requested Circulation		
	(1) Sales through dealers and carriers, street vendors, and counter sales (not mailed)	0	0
	(2) Paid or Requested Mail Subscriptions, (Including advertisers) proof copies and exchange copies	3,500	3,408
c.	Total Paid and/or Requested Circulation (Sum of b (1) and b (2))	3,500	3,408
d.	Distribution by Mail (Samples, complimentary, and other free)	0	0
e.	Free Distribution Outside the Mail (Carriers or other means)	0	0
f.	Total Free Distribution (Sum of d and e)	0	0
g.	Total Distribution (Sum of c and f)	3,500	3,408
h.	Copies Not Distributed		
	(1) Office use, leftovers, spoiled	200	392
	(2) Returned from news agents	0	0
i.	Total (Sum of g, h (1), and h (2))	3,700	3,800
	Percent Paid and/or Requested Circulation (c/g x 100)	100%	100%